RICE UNIVERSITY

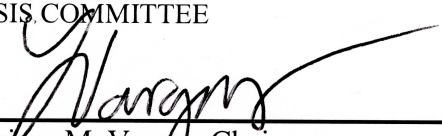## Modeling Polymer Phase Behavior with the Cubic-Plus-Chain (CPC) Equation of State

By

Mohammed M. Alajmi

A THESIS SUBMITTED
IN PARTIAL FULFILLMENT OF THE
REQUIREMENTS FOR THE DEGREE

Master of Science

THESIS COMMITTEE

Francisco M. Vargas, Chair
Louis Owen Assistant Professor
Chemical and Biomolecular Engineering
Rice University

Walter G. Chapman
William W. Akers Professor
Chemical and Biomolecular Engineering
Rice University

Sibani L. Biswal
Associate Professor
Chemical and Biomolecular Engineering
Rice University

HOUSTON, TEXAS
April 2019

ABSTRACT

Modeling Polymer Phase Behavior with the Cubic-Plus-Chain (CPC) Equation of State

By

Mohammed M. Alajmi

Cubic-plus-chain (CPC) equation of state (Sisco et al., *Industrial & Engineering Chemistry Research,* 2019) is used to model vapor-liquid and liquid-liquid phase equilibria for different polymer-solvent systems. Polypropylene (PP), high-density polyethylene (HDPE), low-density polyethylene (LDPE), and polystyrene (PS) polymers are modeled with various solvents. Different factors including solvent effect, molecular weight, pressures, temperatures, polydispersity, and polymer concentration are investigated to study their effects on modeling the phase behavior with the CPC equation of state. CPC modeling results are compared with the Perturbed-Chain Statistical Associating Fluid Theory (PC-SAFT) equation of state and experimental cloud points available in the literature. The CPC equation proved to be capable of modeling the phase behavior for different polymer-solvent systems since it showed good agreement with different experimental cloud points across various temperature ranges. A temperature dependent binary interaction parameter is used in modeling the phase behavior using the CPC equation for polymers as well as different well-defined binary mixtures.

Acknowledgment

I would like first to express my sincere acknowledgment to my thesis advisor Dr. Vargas for everything he has done for me throughout my studies at RICE University. His patience, guidance, motivation, enormous knowledge, and continuous support are what made me continue in academia. Since my first day at the university, Dr. Vargas believed in me and welcomed me to his group, where I met wonderful people. Besides my advisor, I would also like to thank the thesis committee members: Dr. Chapman and Dr. Biswal for their time, feedback, and being part of my thesis committee.

I would like to express my profound gratitude to Dr. Caleb Sisco and Mohammed Abutaqiya. Both of those experts helped me throughout my Master experience at the university. I am also grateful to Kuwait University for believing in me and providing a scholarship for my Master and Ph.D. programs.

Finally, I would like to thank my family for their love and trust in whatever I do, and my brothers Yousef Al-Shamlan and Abdulaziz Alajmi for providing me with continuous encouragement and support.

Contents

List of Figures

List of Tables

Nomenclature

Roman Alphabet

P Pressure

T Temperature

V Volume

A Helmholtz energy

A^R Residual Helmholtz energy

F Reduced residual Helmholtz energy, A^R/RT

n_i Mole number of component i

y_{ij} Mole fraction of component i in phase j

$\hat{f}_i^\alpha$ Fugacity of component i in phase α

K_i Partition coefficient of component i

M_W Weight-average molecular weight

M_n Number-average molecular weight

N_C Number of components

Greek Symbols

α First arbitrary phase

β Reduced volume (for CPC and cubic EOS) or Second Phase

β_c Critical reduced volume

β_j Phase fraction of phase j

μ_i Chemical potential of component i

σ Segment diameter

$\widehat{\phi}_i$ Fugacity coefficient of component i in a mixture

Abbreviations

assoc	Association
att	Attractive
BP	Bubble Pressure
CPC	Cubic-Plus-Chain
CPA	Cubic-Plus-Association
disp	Dispersion
EOS	Equation of State
hs	Hard Sphere
LLE	Liquid-Liquid Equilibrium
mono	Monomer
PR	Peng-Robinson
PC-SAFT	Perturbed-Chain Statistical Associating Fluid Theory
poly	Polymer
RDF	Radial Distribution Function
RK	Redlich-Kwong
rep	Repulsive
SAFT	Statistical Associating Fluid Theory
SRK	Soave-Redlich-Kwong
VDW	Van der Waals
VLE	Vapor-Liquid Equilibrium
VLLE	Vapor-Liquid-Liquid Equilibrium

Chapter 1

Introduction

1.1. Research Motivation

Petrochemicals are chemical products derived from the refining and processing of petroleum, fossil fuels, or even renewable sources. These chemical compounds composed mainly of hydrogen and carbon, and they are used in various industrial and commercial purposes. There are two main categories of petrochemicals. The first category is alkenes, which is also called olefins, that consists of unsaturated hydrocarbon with at least one double bond between the carbon atoms. Some of the major petrochemicals in the alkene class are ethylene, propylene, and butylene. The ethylene chemical compound can be transformed into polyethylene by the polymerization reaction. The double bond of ethylene consists of σ and π bonds, and the σ bond is stronger than the π bond; therefore, the polymerization reaction breaks the π bonds for many ethylene monomers leading to produce a long stronger chain of repeated $(-CH_2 - CH_2-)$ units. Polypropylene can be produced by polymerization of propylene in the same manner.

The second petrochemical class is aromatics, and the major compounds in this group are benzene, toluene, ethylbenzene, and styrene. Ethylbenzene is made from ethylene and benzene ring by an acid-catalyzed chemical reaction. Styrene is made from dehydrogenation of ethylbenzene. Polystyrene can be produced by the polymerization of styrene and breaking the π bond to form a strong σ bond between the monomers to produce polystyrene polymer. More details on the polymerization of polyethylene, polypropylene, and polystyrene are presented in this work.

There are different methods to produce both of these petrochemicals' classes. They can be produced by petroleum refineries and chemical plants through thermal cracking, fluid catalytic cracking (FCC), steam cracking of natural gas condensate, and catalytic reforming of naphtha.[1] Fluid catalytic cracking (FCC) is used to convert crude oil with high hydrocarbon molecular weight to more beneficial products. FCC replaces the thermal cracking because it produces more alkenes and gasoline, which leads to a higher economic rate.

These petrochemicals can be used in many different purposes. For example, ethylene and propylene can be polymerized to form polyethylene and polypropylene that are important in clothing, medical, and plastics productions.[2,3] In general, petrochemicals involve in producing soaps, solvents, drugs, pesticides, rubber, films, paints, plastics, clothes, automobiles, and even aircraft. These useful economical applications are what makes the researchers and industries targeting the petrochemicals and studying them diligently in order to maximize their productions.

1.2. Problem Statement

Many researchers have been investigating intensively on the phase behavior of many different chemical solutions. The main focus is targeting the complex mixtures and how to describe their phase behavior whether it is vapor-liquid equilibrium (VLE), liquid-liquid equilibrium (LLE), or solid-liquid equilibrium (SLE). These phase equilibria were investigated by studying the equations of state and their associated mixing rules.

The broad aim of this work is to use a new equation of state proposed by Sisco et al[4], which is the cubic-plus-chain (CPC) equation of state, to model the phase behavior of different petrochemical compounds with different solvents. This equation of state derived from hybridizing the cubic equation of state with the chain term from the Statistical Associating Fluid Theory (SAFT) equation of state proposed by Chapman et al[5,6]. The main reason for modeling the phase equilibrium of these compounds is the lack of experimental data available in the literature for wide ranges of temperature and compositions. Another reason is the lack of accuracy in the phase behavior prediction of different equations of state in modeling polymers. Hence, the goal is to find a simple and robust equation of state that can accurately model the phase behavior of different polymers with different solvents' type whether the solvents are in the alkane, cyclic, aromatic, or even in the alkene family.

Cubic-plus-chain (CPC) equation of state is a new equation of state, and it was not tested intensively in modeling polymer. Therefore, it is crucial to determine the parameters for each polymer systems and the factors that affect these parameters in order to accurately predicts the equilibrium behavior and to create a reliable parameters database for

systems consisting of different polymers with different solvents. Moreover, a comparison of the CPC equation with different equations of state needs to be performed in order to compare the accuracy, speed, and simplicity. Also, the comparison is necessary to check which model matches the experimental data available in the literature for different systems.

1.3. Thesis Outline

There are four different chapters in this work. This chapter addresses the introduction of the thesis along with the problem statement and the thesis outline. Chapter 2 presents the conditions and the restrictions for the phase equilibrium starting with stating the thermodynamics property relations and deriving the equilibrium conditions by using those relations. In addition, different formulations of equilibrium conditions in terms of fugacity and fugacity coefficient are addressed. It also presents the most commonly used equations of state framework associated with modeling the phase behavior of hydrocarbon systems. Starting with the derivation of the first equation of state, and this equation is known as the ideal gas equation of state. After that, the cubic equation of state will be addressed in detail for four different cubic equation of states models starting with the first cubic equation of state, which is Van der Waals equation of state. Then, Statistical Associating Fluid Theory (SAFT) equation of state is presented along with the associated equations. After that, both the cubic-plus-association (CPA) and the cubic-plus-chain (CPC) equations of state are addressed in detail in different forms as well as mixing and combining rules used in those equations.

Chapter 3 presents the phase behavior of polymer-solvent systems with using the CPC equation of state. The modeling technique and different approaches in identifying pure component parameters are discussed in detail. Polypropylene, high-density polyethylene (HDPE), low-density polyethylene (LDPE), and polystyrene (PS) systems are modeled with different solvents. The effect of different factors including temperature, molecular weight, polydispersity, and polymer concentration are shown in this chapter. A temperature dependent binary interaction parameter in modeling polymer systems and 15 well-defined systems are discussed in this chapter.

Chapter 4 concludes the thesis by stating the final results for modeling polymer systems with the CPC equations of state, and how different factors affect the modeling results. Additionally, it proposes some future work recommendations in adjusting the CPC equation of state in modeling phase equilibrium for different systems.

Chapter 2

A Review on Phase Equilibrium and Equation of State Models

2.1. Introduction

The term equilibrium for a given system means that there is no change exists in the properties of this system with changing the time. There are different types of equilibria. For example, the chemical equilibrium means that the net change in the concentrations of the reactants and products is zero, which means that the reactants and products concentration does not change with changing the time. However, phase equilibrium means the equilibrium between different phases such as vapor, liquid, and solid of a pure component or mixture. Phase equilibrium can be modeled using different equations of state.

Equation of state is a thermodynamic equation that states the relationship between pressure, volume, and temperature in order to calculate the state variables such as enthalpy, entropy, and internal energy. Equations of state can be applied to describe phases behavior whether the phases are gases, liquids, or even solids. However, the

accuracy varies from one equation of state to another for the description of these phases whether they are a pure component or a mixture. Therefore, different equations of state have been proposed along with different mixing rules. Equations of state can be used to predict and model equilibrium phase behavior for pure component or even mixtures. It can be used to predict the saturation pressure in many phase equilibrium conditions. Some of these equilibrium behaviors are vapor-liquid equilibrium (VLE), liquid-liquid equilibrium (LLE), solid-liquid equilibrium (SLE), or even vapor-liquid-liquid equilibrium (VLLE).

In this chapter, the condition and relation between the physical and chemical properties of mixtures at equilibrium are stated. In addition, the ideal gas equation of state, cubic equations of state, Statistical Associating Fluid Theory (SAFT), cubic-plus-association (CPA) equation of state, and cubic-plus-chain (CPC) equation of state are addressed in some detail along with the associated mixing rules. Some of these equations are represented in pressure form (P) as well as reduced residual Helmholtz function (F) form.

2.2. Thermodynamic Functions and Equilibrium State

The fundamental property relations are thermodynamic equations that give expression to calculate Helmholtz energy (A), enthalpy (H), internal energy (U), and Gibbs energy (G). The fundamental property relations are state function since they follow Legendre Transformation, and they have exact differentials. A state function means that these properties is path independent function. Legendre Transformation[7] formula is given by:

$$g = f - x \left(\frac{\partial f}{\partial x}\right)_y \qquad (2.1)$$

Where g is a new state function calculated from f, which is another state function. For example, the Legendre Transformation can be used to derive Helmholtz energy from the internal energy. Moreover, Gibbs energy can be derived from the enthalpy equation. The fundamental property relations for mixtures can be expressed as follows:

$$dU\left(S, V, n_1, \ldots, n_{N_C}\right) = TdS - PdV + \sum_{i=1}^{N_C} \mu_i \, dn_i \qquad (2.2)$$

$$dH\left(P, S, n_1, \ldots, n_{N_C}\right) = VdP + TdS + \sum_{i=1}^{N_C} \mu_i \, dn_i \qquad (2.3)$$

$$dG\left(T, P, n_1, \ldots, n_{N_C}\right) = -SdT + VdP + \sum_{i=1}^{N_C} \mu_i \, dn_i \qquad (2.4)$$

$$dA\left(V, T, n_1, \ldots, n_{N_C}\right) = -PdV - SdT + \sum_{i=1}^{N_C} \mu_i \, dn_i \qquad (2.5)$$

Where n_i is the mole number for component i, μ_i is the chemical potential for component i, and N_C is the number of components in a mixture. These thermodynamic functions show that temperature, volume, pressure, and entropy can be calculated from more than one equation. Therefore, the calculation of these properties is not restricted to one equation and can be calculated from another equation depends on the available data for these properties. For example, pressure can be calculated from equations (2.2) and (2.5). Temperature can be calculated from equation (2.2) and equation (2.3). Volume can be

expressed by both of equation (2.3) and equation (2.4). Similarly, entropy can be calculated by using equation (2.4) and equation (2.5).

In other words, pressure, temperature, volume, and entropy can be expressed as follows:

$$P = -\left(\frac{\partial A}{\partial V}\right)_{T,n} = -\left(\frac{\partial U}{\partial V}\right)_{S,n} \tag{2.6}$$

$$T = \left(\frac{\partial H}{\partial S}\right)_{P,n} = \left(\frac{\partial U}{\partial S}\right)_{V,n} \tag{2.7}$$

$$V = \left(\frac{\partial H}{\partial P}\right)_{S,n} = \left(\frac{\partial G}{\partial P}\right)_{T,n} \tag{2.8}$$

$$S = -\left(\frac{\partial A}{\partial T}\right)_{V,n} = -\left(\frac{\partial G}{\partial T}\right)_{P,n} \tag{2.9}$$

These equations prove that these thermodynamics properties can be expressed and transformed through mathematical relations. Furthermore, it is noticeable that chemical potential (μ_i) for each component whether pure or in a mixture can be calculated from all of the fundamental property relations, which are equations (2.2) through (2.5).

The conditions for chemical equilibrium can be derived from re-arranging equation (2.2) in terms of entropy to give:

$$dS(U,V,n_1,\dots,n_{N_C}) = \frac{1}{T}dU + \frac{P}{T}dV - \frac{1}{T}\sum_{i=1}^{N_C} \mu_i dn_i \tag{2.10}$$

The previous equation represents the change in entropy, and this change should be zero at equilibrium for an isolated system according to the second law of thermodynamics. The change is zero since the entropy reaches a maximum constant value at equilibrium for an isolated system. In order to determine the equilibrium conditions, let's consider

having two phases (α) and (β). If those two phases for different components contained in an isolated system, which there is neither energy nor mass can enter or escape the system, equation (2.10) can be re-written as:

$$dS = \frac{P^\alpha}{T^\alpha} dV^\alpha - \frac{1}{T^\alpha} \sum_{i=1}^{N_C} \mu_i^\alpha dn_i^\alpha - \frac{P^\beta}{T^\beta} dV^\alpha + \frac{1}{T^\beta} \sum_{i=1}^{N_C} \mu_i^\beta dn_i^\alpha = 0 \qquad (2.11)$$

More details in deriving equation (2.11) are shown in Appendix A. In order to satisfy this equation, the temperature, pressure, and chemical potentials for both phases need to be equal. Therefore, the conditions at equilibrium should be:

$$T^\alpha = T^\beta = \cdots = T^\pi \qquad (2.12)$$

$$P^\alpha = P^\beta = \cdots = P^\pi \qquad (2.13)$$

$$\mu_i^\alpha = \mu_i^\beta = \cdots = \mu_i^\pi \qquad (2.14)$$

Where μ_i is the chemical potential for component i, and $\alpha, \beta, \dots, \pi$ are the phases at equilibrium. For example, if there is vapor-liquid equilibrium, T^V must be equal to T^l at equilibrium. Similar concept applies for the pressure and chemical potential. The phase equilibrium can be expressed by fugacity ($\hat{f}$) instead of chemical potential since they are related through the following equation:

$$d\mu_i = RT \, d(\ln \hat{f}_i) \qquad (2.15)$$

And if the relation between the fugacity and chemical potential is integrated from a reference pressure state to a final state, it gives the following expression:

$$\mu_i^\beta(T, P^\beta) = \mu_i^\alpha(T, P^\alpha) + RT \ln \frac{\hat{f}_i^\beta(T, P^\beta)}{\hat{f}_i^\alpha(T, P^\alpha)} \tag{2.16}$$

However, the temperature and pressure are equivalent in the equilibrium condition for all phases; therefore, the second term of the previous equation goes to zero and the equal chemical potential relation is restored. Since the fugacity in the second term is equal at the same pressure and temperature in all phases; thus, the equilibrium condition in terms of fugacity can be expressed as follows:

$$\hat{f}_i^\alpha = \hat{f}_i^\beta = \cdots = \hat{f}_i^\pi \tag{2.17}$$

Again, π is the number of phases, and N_C is the number of components in the mixture. The fugacity is related to the fugacity coefficient through the following equation:

$$\hat{f}_i(T, P, n) = y_i \hat{\phi}_i P \tag{2.18}$$

Where y_i is the mole fraction for component i in the mixture, P is the pressure, and $\hat{\phi}_i$ is the fugacity coefficient in the mixture. The fugacity coefficient of component i in a mixture can be calculated by:

$$RT \ln \hat{\phi}_i(T, P, n) = \left(\frac{\partial A^R}{\partial n_i}\right)_{T,V,n_{j \neq i}} - RT \ln Z \tag{2.19}$$

In the previous equation, Z is the compressibility factor, R is the gas constant, T is the temperature, and A^R is the residual Helmholtz energy. Fugacity coefficient as well as the residual Helmholtz energy can be calculated by equations of state. Different residual Helmholtz energy equations are discussed in this chapter for various equations of state.

Moreover, the phase equilibrium calculations require material balance constraints to be added to the equilibrium conditions mentioned earlier in equations (2.12) to (2.14). For instance, if the system consists of components in α and β phases that are at equilibrium, a partition coefficient that relates the two phases is given by:

$$K_i \equiv \frac{y_i^\alpha}{y_i^\beta} \qquad (2.20)$$

This partition coefficient works as an indication of the tendency of the species to favor one phase over the other phase. For example, if the K_i value is larger than one, then the component i has a higher concentration in the α phase over the β phase, and vice versa.

If equation (2.18) is used in equation (2.20), it gives the following modified expression for K_i:

$$K_i = \frac{\hat{f}_i^\alpha}{\hat{f}_i^\beta} \frac{\hat{\phi}_i^\beta}{\hat{\phi}_i^\alpha} \frac{P}{P} = \frac{\hat{\phi}_i^\beta}{\hat{\phi}_i^\alpha} \qquad (2.21)$$

The fugacity in the equation above needs to be canceled because of the equal fugacity condition at equilibrium as stated in equation (2.17). The fugacity coefficient formula depends on the choice of the equation of state, and these equations of state will be reviewed intensively in this chapter along with their associated mixing rules.

Additional equilibrium constraints to satisfy the material balance for the non-reacting system are the sum of phase fractions for each phase is equal to one. Moreover, the sum of mole fractions of all components in a specific phase is equal to one as well. These two constraints can be expressed as follows:

$$\sum_{j=\alpha}^{\pi} \beta_j = 1 \tag{2.22}$$

$$\sum_{i=1}^{N_C} y_i^\alpha = 1 \tag{2.23}$$

Where β_j is the phase fraction of phase j. Additional constraint for the phase equilibrium is given by the following expression:

$$z_i = \sum_{j=\alpha}^{\pi} \beta_j y_{ij} \tag{2.24}$$

Where z_i is the overall composition for component i, y_{ij} is the mole fraction for component i in phase j. In other words, the previous equation states the constraint where the sum of phase fraction times the mole fraction for component i in all of the phases involved in the equilibrium is equal to the overall composition for this component.

2.3. Equations of State Models and Applications

2.3.1. Ideal Gas

The ideal gas law was discovered by Émile Clapeyron[8] by combining four different laws. The first law is Boyle's law that describes the relationship between the pressure (P) and the volume (V) at constant temperature (T). This law states that the pressure of a gas increases when the volume of the container decreases. It can be mathematically expressed as follows:

$$P \propto \frac{1}{V} \tag{2.25}$$

The second law is Charles's law that describes the effect of gases temperature on the volume. This law describes how gases have expansion tendency when there is heat applied to the system at constant pressure. This law can be stated as:

$$V \propto T \tag{2.26}$$

The third law is Avogadro's law that relates the amount of the gas component to the volume of the gas. For example, if hydrogen and nitrogen have the same volume at constant pressure and temperature, they will have the same amount of molecules (n). The relationship between the volume and the amount of the gas is given by the following expression:

$$V \propto n \tag{2.27}$$

The last law is Gay-Lussac's law that describes the relationship between the pressure and the temperature of gases. The pressure of a gas is directly proportional to the temperature if the volume and the mass of the gas are constant. If the pressure of the gas at a fixed mass and volume increases, the temperature increases. The mathematical expression of this law is given by:

$$P \propto T \tag{2.28}$$

By combining all of these four laws and absorbing their constants by the gas constant called R, the ideal gas law for diluted gases is expressed as follows:

$$P = \frac{nRT}{V} = \frac{RT}{\hat{V}}$$ (2.29)

Where P is the gas pressure, T is the temperature, V is the volume, n is the number of moles, R is the gas constant in units of energy per temperature increment per mole, and $\hat{V}$ is the molar volume in units of volume per mole.

The ideal gas law was the first equation of state formed to relate the pressure, temperature, and volume of the gases. This equation of state is suitable for diluted gases with low pressure. This law is based on the assumptions that the gas molecules are far apart without exerting forces on one another, they have an extremely small volume related to the total volume of the system, and they collide with the container walls elastically with a negligible duration. However, the ideal gas equation fails to describe the gases with high pressure and moderate temperature since the interaction between the molecules are considered and that violates the ideal gas assumption. Consequently, this equation of state cannot describe the pressure, temperature, and volume for the real gases, liquid, and solids. Therefore, more complex equations of state need to be used to perform the pressure, volume, and temperature calculations.

2.3.2. Cubic Equation of State

The ideal gas equation of state was not capable of representing the pressure, volume, and temperature for both liquids and real gases. Hence, there were many significant

researches to create a better equation that can extend the use of the equation of state to account for vapors and liquids. Cubic equations of state were proposed to account for both the attraction and repulsion molecular interactions. It is called cubic because it can be written as a cubic function in terms of volume. Cubic equations of state are widely used in many industrial software packages because of their generality, simplicity, acceptable speed, and adequate accuracy in many different applications.

There are many remarkable efforts in improving cubic equations of state, and the first practical equation of this form was proposed by Johannes van der Waals[9]. The van der Waals equation of state was the first equation that can model vapor-liquid equilibrium and liquid-liquid equilibrium for complex components and mixtures. Van der Waals equation in the pressure and volume forms are given by:

$$P = \frac{nRT}{V - B} - \frac{A}{V^2} \tag{2.30}$$

$$V^3 - \left(B + \frac{nRT}{P}\right)V^2 + \frac{A}{P}V - \frac{AB}{P} = 0 \tag{2.31}$$

It is noticeable that the equation is cubic in terms of volume. It is important to realize that cubic equations of state were developed for pure components not for mixtures, and they will fail when they are applied for mixtures. Thus, mixing rules were proposed to enhance the prediction of these cubic equations of state. Some of the mixing rules were tested for a wide range of pressure and temperature to accurately predict the vapor-liquid equilibrium for different mixtures. Both of A and B can be calculated by using the following mixing rules:

$$A = \sum_i \sum_j n_i n_j \sqrt{a_i a_j}(1 - k_{ij}) \tag{2.32}$$

$$B = \sum_i n_i b_i \tag{2.33}$$

The mixing rules above were used to average the pure component parameters (a_i) and (b_i), which are interaction energy and excluded volumes of the components. Equations (2.35) and (2.36) shows the expressions for calculating a_i and b_i parameters. If both of A and B are zero, the cubic equations of state will be reduced to the ideal gas equation.

Different contributions for different cubic equations of state were done based on the van der Waals equation. These modifications were done for the second term of van der Waals equation, which is the attractive term. The first modification is called Redlich-Kwong (RK)[10] equation of state. This adjustment improves the prediction of the vapor physical properties. A major drawback is the RK equation fails to predict the liquid phase accurately. Therefore, it does not correctly predict the vapor-liquid equilibrium (VLE) and liquid-liquid equilibrium (LLE).

A new temperature dependence parameter (α) and Pitzer's acentric factor (ω_i) were introduced to account for the shape of molecules and to accommodate the prediction away from the critical point. These parameters were proposed by Soave. Therefore, another equation of state was developed to account for both vapor and liquid that is Soave-Redlich-Kwong (SRK)[11] equation of state. There is a drawback in this equation of state. It does not predict the liquid density correctly, and the molar volume are

overestimated. After that, Peng-Robinson (PR)[12] equation of state was proposed to account for both vapor and liquid near equilibrium conditions. However, (SRK) equation of state predicts polar system better than (PR) equation of state.

A generic cubic equation of state that accounts for different cubic EOS forms including van der Waals, Redlich-Kwong (RK), Soave-Redlich-Kwong (SRK), and Peng-Robinson (PR) equations of state is given by:

$$P = \frac{nRT}{V - B} - \frac{A}{(V + \delta_1 B)\,(V + \delta_2 B)} \tag{2.34}$$

The parameters (δ_1) and (δ_2) for van der Waals, RK, SRK, and PR equations in the generic form is given in **Table 2.1**. Van der Waals equation of state can be reduced by having both of δ_1 and δ_2 to be zero. The pure component interaction energy (a_i) and excluded volume (b_i) are calculated as follows:

$$a_i = \Omega_a \frac{R^2 T_c^2}{P_c} \alpha \tag{2.35}$$

$$b_i = \Omega_b \frac{R T_c}{P_c} \tag{2.36}$$

where Ω_a and Ω_b are constants tuned to match the critical point, T_c is the critical temperature, and P_c is the critical pressure. The values for Ω_a and Ω_b for four different cubic equations of state are given in **Table 2.1**.

Table 2.1. Parameter Values for Selected Cubic Equations
of State

EOS	δ_1	δ_2	Ω_a	Ω_b
van der Waals	0	0	0.42188	0.12500
RK	1	0	0.42748	0.08664
SRK	1	0	0.42748	0.08664
PR	$1 + \sqrt{2}$	$1 - \sqrt{2}$	0.45724	0.07780

In **Table 2.1**, different values of δ_1, δ_2, Ω_a, and Ω_b for four cubic equations of state are given. Van der Waals equation of state does not depend on δ_1 and δ_2 parameters whereas the other three equations of state require those parameters. The temperature dependent parameter (α) is given in **Table 2.2**.

Table 2.2. Tempereture Dependent Paramter Values for
Selected Cubic Equations of State

EOS	$\kappa(\omega)$	α
van der Waals	NA	1
RK	NA	$\sqrt{T_c/T}$
SRK	$0.480 + 1.574\omega - 0.176\omega^2$	$\left[1 + \kappa\left(1 - \sqrt{T/T_c}\right)\right]^2$
PR	$0.37464 + 1.54226\omega - 0.26992\omega^2$	$\left[1 + \kappa\left(1 - \sqrt{T/T_c}\right)\right]^2$

In general, equations of state are commonly written in pressure form as in van der Waals equation and the generic cubic equation of state mentioned earlier in this section, or in residual Helmholtz form (A^R) that can be expressed as follows:

$$A^R(T,V,n) = -\int_{\infty}^{V}\left(P - \frac{nRT}{V}\right)dV \tag{2.37}$$

The above expression can be used to express any other thermodynamics properties by the differentiation of residual Helmholtz energy and the reduced residual Helmholtz function (F). Therefore, it is very useful to express equations of state in these forms. The reduced residual Helmholtz function form of the cubic equation of state is given by using the above relation to integrate the pressure equation to give the following expressions:

$$F = \frac{A^R(T,V,n)}{RT} = a^{rep} + a^{att} \tag{2.38}$$

$$a^{rep} = -n\,ln(1-\beta) \tag{2.39}$$

$$a^{att} = -\frac{A}{BRT(\delta_1 - \delta_2)}\,ln\frac{1+\delta_1\beta}{1+\delta_2\beta} \tag{2.40}$$

Where β is the reduced volume, and it is the ratio of B to V. Both of a^{rep} and a^{att} in the equations above are the repulsive and the attractive terms, respectively.

2.3.3. PC-SAFT Equation of State

In 1989, Chapman et al. proposed an equation of state that uses Wertheim's[13–16] thermodynamic perturbation theory, and this equation is called the Statistical Associating Fluid Theory (SAFT)[5,6]. The SAFT equation uses a reference fluid of hard spheres. These hard spheres can bond by covalent bonds in order to create chains, and these chains have terminal sites that can bond by hydrogen bonding with different

chains. The hard spheres in the chains can interact through weak dispersion forces.
Figure 2.3.1 depicts the SAFT model starting from hard spheres.
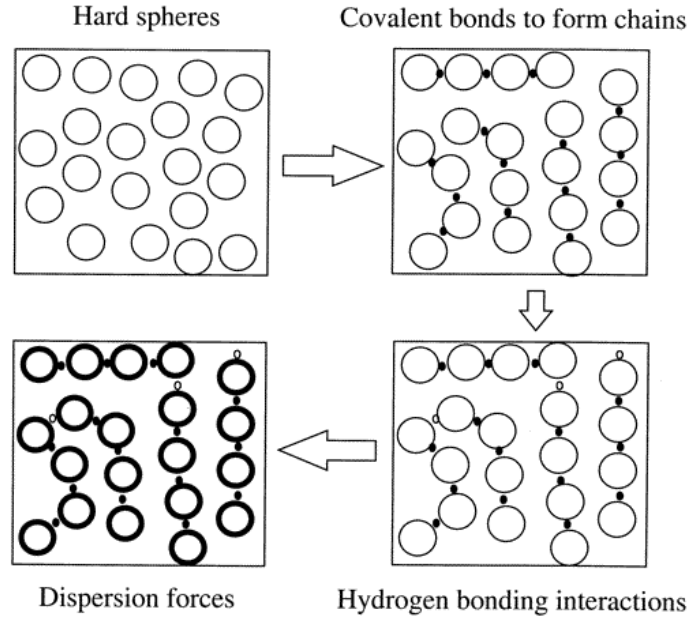
Figure 2.3.1: Schematic representation of the physical basis of SAFT model [17]

The reduced residual Helmholtz function for the SAFT equation of state can be written as follows:

$$F = \frac{A^R(T, V, \boldsymbol{n})}{RT} = a^{hs} + a^{chain} + a^{assoc} + a^{disp} \tag{2.41}$$

Where a^{hs} is the hard sphere term, a^{chain} is the chain term, a^{assoc} is the association term, and a^{disp} is the dispersion term.

Many researchers proposed modifications to this equation of state but with retaining the fundamental form, and some others changed the form by adding or dropping terms of the original SAFT equation. Huang and Rodosz[18] version of SAFT equation of state, which was initially proposed by Chapman et al., is the most common form of SAFT equation that is

being used by many researchers at that time. Then, Gross and Sadowski introduced another version of the SAFT equation of state, which is perturbed-chain SAFT (PC-SAFT)[19-22]. PC-SAFT equation of state proved to be very accurate in modeling phase equilibrium behavior for complex mixtures. PC-SAFT was developed by applying Baker and Henderson[23-25] perturbation theory to a hard-chain reference fluid.

The difference between the PC-SAFT equation and the SAFT equation is that SAFT equation uses hard-spheres as a reference; however, PC-SAFT uses the dispersion term for a hard-chains system. In addition, the pair potential for PC-SAFT is different than the one that is being used in the SAFT equation. PC-SAFT uses the pair potential proposed by Chen and Kreglewski[26], and is given as follows:

$$u(r) = \begin{cases} \infty & r < (\sigma - s_1) \\ 3\epsilon & (\sigma - s_1) \leq r < \sigma \\ -\epsilon & \sigma \leq r < \lambda\sigma \\ 0 & r \geq \lambda\sigma \end{cases} \tag{2.42}$$

Where $u(r)$ is the pair potential, r is the radial distance between both segments, λ is the reduced well width, and σ is the temperature-independent segment diameter.

Mansoori et al.[27] introduced an expression for a mixture of hard-spheres, and Chapman developed the chain term in order to describe the interactions of the spheres in infinite attraction limits. The expressions for chain term and hard sphere (hs) are given by:

$$a^{chain} = -\sum_{i=1}^{N_C} n_i (m_i - 1) \ln g_{ii}^{hs}(\sigma_{ii}) \tag{2.43}$$

$$a^{hs} = \frac{6}{\pi\tilde{\rho}} \left[\frac{3\zeta_1\zeta_2}{1 - \zeta_3} + \left(\frac{\zeta_2{}^3}{\zeta_3{}^2} - \zeta_0 \right) \ln(1 - \zeta_3) + \frac{\zeta_2{}^3}{\zeta_3(1 - \zeta_3)^2} \right] \tag{2.44}$$

$$\zeta_n = \frac{\pi}{6}\tilde{\rho}\sum_{i=1}^{N_C} n_i m_i d_i^n \tag{2.45}$$

Where m is the number of monomer segments in the chain of component i, ζ_n are size parameter, and $\tilde{\rho}$ is the number density. Moreover, g_{ij}^{hs} is the radial pair distribution function, and d_{ij} is an average segment diameter for component i and j. Both of these parameters can be expressed as follows:

$$g_{ij}^{hs} = \frac{1}{1-\zeta_3} + d_{ij}\left[\frac{3\zeta_2}{(1-\zeta_3)^2}\right] + d_{ij}^2\left[\frac{2\zeta_2^2}{(1-\zeta_3)^3}\right] \tag{2.46}$$

$$d_i = \sigma_i\left[1 - 0.12\,exp\left(-\frac{3\epsilon_i}{kT}\right)\right] \tag{2.47}$$

The association term in terms of the unbonded monomer fraction at site A of component i is given by:

$$a^{assoc} = \sum_i^{N_C} n_i \sum_{A_i}^{S(i)}\left[ln\,X^{A_i} - \frac{1}{2}X^{A_i} + \frac{1}{2}\right] \tag{2.48}$$

Where N_c and $S(i)$ are the number of components and the total number of associating sites on molecule i, respectively. X^{A_i} is the unbonded monomer fraction at site A.

The dispersion term for PC-SAFT was developed by using an extension of Barker-Henderson perturbation theory[23-25]. The dispersion term with using the van der Waals one-fluid mixing rule is expressed as follows:

$$a^{disp} = a_1 + a_2 \tag{2.49}$$

$$a_1 = -2\pi\tilde{\rho}\, I_1 \sum_i \sum_j n_i n_j m_i m_j \left(\frac{\epsilon_{ij}}{kT}\right) \sigma_{ij}{}^3 \tag{2.50}$$

$$a_2 = -\pi\bar{m}\tilde{\rho}C_1 I_2 \sum_i \sum_j n_i n_j m_i m_j \left(\frac{\epsilon_{ij}}{kT}\right)^2 \sigma_{ij}{}^3 \tag{2.51}$$

Where I_1 and I_2 are power series in reduced density, C_1 is a compressibility coefficient, m_i is the number of monomer segments in the chain i, and $\bar{m}$ is used to account for the mixture. I_1 and I_2 expressions are given by:

$$I_1 = \sum_{i=0}^{6} a_i \eta^i \tag{2.52}$$

$$I_2 = \sum_{i=0}^{6} b_i \eta^i \tag{2.53}$$

Where η^i is the reduced density, and the coefficients a_i and b_i are constants depend on the chain length. The combining rules for σ_{ij} and ϵ_{ij} are given by:

$$\sigma_{ij} = \frac{1}{2}(\sigma_i + \sigma_j) \tag{2.54}$$

$$\epsilon_{ij} = \sqrt{\epsilon_i \epsilon_j}\,(1 - k_{ij}) \tag{2.55}$$

These combining rules apply when there is a pair of unlike segments, and k_{ij} is a binary interaction parameter that correct the interactions between segments of unlike chains. Therefore, PC-SAFT equation depends on three major parameters, which are segment number (m), segment diameter (σ), and segment energy parameter (ϵ/k).

2.3.4. CPA Equation of State

Kontogeorgis et al.[28] proposed a new version of equations of state that combines the cubic equation of state and the theoretical background of the perturbation theory for chemical association part. This equation of state is called Cubic Plus Association (CPA), and it can describe the associating fluids. The choice of the cubic equation of state in the CPA equation depends on the researchers; however, it was initially designed based on SRK equation of state and the association term from the SAFT equation of state. The CPA equation of state in the pressure form is given by:

$$P = \frac{nRT}{V - B} - \frac{A}{V(V + b)} + \frac{nRT}{V} \rho \sum_A \left[\frac{1}{X^A} - \frac{1}{2}\right] \frac{\partial X^A}{\partial \rho} \qquad (2.56)$$

Where the first two terms are from SRK equation of state, and the third term is from the SAFT equation of state. The CPA equation of state gives the physical contribution by the cubic terms, and it gives the chemical contribution by the association term. The reduced residual Helmholtz function for CPA is expressed as follows:

$$F = \frac{A^R(T,V,n)}{RT} = a^{rep} + a^{att} + a^{assoc} \qquad (2.57)$$

Where a^{rep} is the repulsive contribution, a^{att} is the attractive contribution, and a^{assoc} is the association term. The a^{rep}, a^{att}, and a^{assoc} are given in equations (2.39), (2.40), and (2.48), respectively. Similarly, the first two terms are from the cubic equation of state, and the association term is obtained from the PC-SAFT equation of state with some modifications in the radial distribution function and energy parameter. These parameters are given by:

$$g_{ij}^{CPA} = \frac{1}{1 - 1.9\eta} \tag{2.58}$$

$$\eta = \left(\frac{1}{4V}\right) B \tag{2.59}$$

$$a(T) = a_0 \left[1 + c_1 \left(1 - \sqrt{T_r}\right)\right]^2 \tag{2.60}$$

where g is the modified radial distribution function for CPA, η is the reduced fluid density, a is the energy parameter, and T_r is the reduced temperature given by T/T_c. The physical contribution by the cubic equation depends on three parameters that need to be tuned, and these parameters are a_0, B, and c_1.

A major drawback of this equation of state is that it loses the ability to be cubic in terms of volume. Moreover, this equation of state requires five parameters to be fit to liquid density and vapor pressure data. These parameters are a_0, B, c_1, ϵ^{AB}, and β^{AB}. The first three parameters are originally from the physical part of the equation, and the last two parameters are from the association part. In addition, the CPA equation requires X^A to converge, and that is done by using an optimization routine inside the volume solver. This routine makes the equation more time consuming than the cubic models. There are four different approaches used to estimate these parameters. These approaches are: global estimation, three-parameter estimation, estimation through the homomorph approach, and optimization based solely on vapor pressures.[28] CPA equation of state enhances the liquid volume predictions because of the association term and the number of the parameters used in this equation of state. There are many efforts in applying the CPA equation to many different systems, and it showed good result in modeling phase behavior for polar compounds and crude oils[29-35]. There are some modifications to this

equation of state to lower down the number of parameters used, and these adjustments proved to have an excellent correlation to vapor pressure and liquid volume.

2.3.5. CPC Equation of State

The cubic-plus-chain (CPC)[4] equation of state is a new equation that hybridizes the standard cubic equations of state with a chain term from the SAFT equation. The addition of the chain term in the CPC equation accounts for the change in the energy because of the chain formation. **Figure 2.3.2** illustrates a comparison between the cubic equation of state molecule and the CPC equation molecules in the chain.

(A)   **(B)**
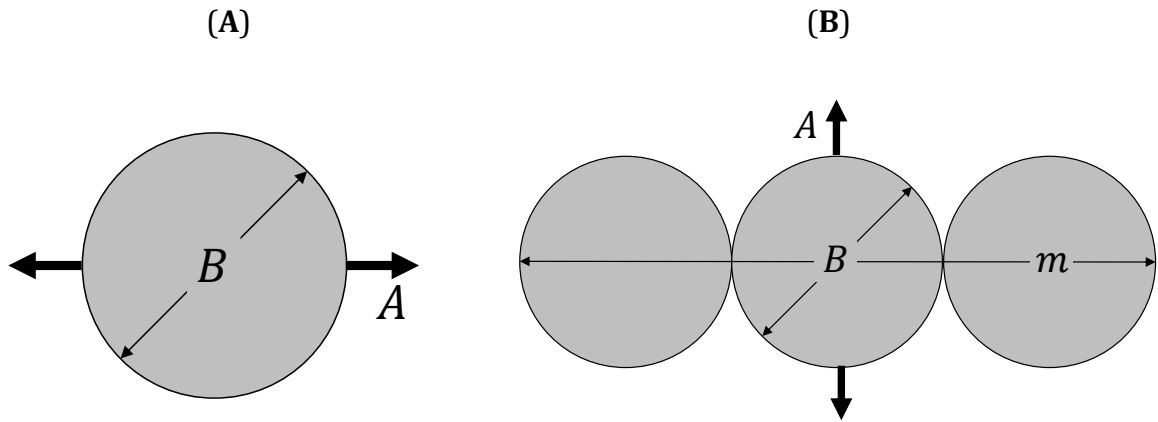
Figure 2.3.2*: (**A**) model representation of a molecule for cubic EOS. (**B**) model representation of a molecule in a chain for CPC[4].*

The CPC equation of state in terms of pressure is given by combining RK equation of state, which is reformulated as a function of chain length, with the chain term from SAFT equation of state as follows:

$$P = \frac{nRT}{V}\left(1 + \frac{\overline{m}^2 B}{V - \overline{m}B}\right) - \frac{\overline{m}^2 A}{V(V + \overline{m}B)} - nRT\frac{\overline{m}B}{V^2}\left[\sum_i^{N_C} n_i(m_i - 1)\frac{g'(\beta)}{g(\beta)}\right] \qquad (2.61)$$

Where A and B parameters are the interaction energy and the excluded volume, respectively. Moreover, $\bar{m}$ is the average chain length or segment number, β is the reduced volume, and $g(\beta)$ is the radial distribution function. The reduced volume and the radial distribution function can be expressed by:

$$\beta = \frac{\bar{m}B}{V} \tag{2.62}$$

$$g(\beta) = \frac{1}{1 - 0.475\beta} \tag{2.63}$$

The radial distribution function shown above is proposed by Elliott et al.[36] The mixing rules for the interaction energy (A) and the excluded volume (B) are given by:

$$\bar{m} = \sum_i x_i m_i \tag{2.64}$$

$$A = \frac{1}{\bar{m}^2} \sum_i \sum_j n_i n_j m_i m_j a_{ij} \tag{2.65}$$

$$B = \frac{1}{\bar{m}} \sum_i n_i m_i b_{ii} \tag{2.66}$$

If the value of m_i in the previous equations sets to be equal to one, then the mixing rule for the CPC equation matches the ones for the standard cubic equation of state. The combining rules for both a_{ij} and b_{ij} are expressed as follows:

$$a_{ij} = \sqrt{a_i a_j}(1 - k_{ij}) \tag{2.67}$$

$$b_{ij} = \frac{1}{2}(b_i + b_j) \tag{2.68}$$

The parameters a_i and b_i can be calculated by using the expressions in (2.35) and (2.36); however, the parameter Ω_a and Ω_b in those equations are re-adjusted in terms of the chain length m, and they are given by:

$$\Omega_a(m) = \frac{1}{m^2}\left[\frac{\beta_c Z_c^2}{\lambda^{mon}} + (m-1)\beta_c Z_c \frac{\lambda^{chain}}{\lambda^{mon}}\right] \tag{2.69}$$

$$\Omega_b(m) = \frac{1}{m}\beta_c Z_c \tag{2.70}$$

The equations for calculating β_c and Z_c are shown in detail in Appendix A. The parameters a_i and b_i in CPC are calculated from the critical properties (T_C and P_C) for each component, and the parameter m_i is tuned to match saturation pressure and liquid density. However, the PC-SAFT parameters were tuned to match the saturation pressure and liquid density not the critical point.

Cubic Plus Chain equation of state can be expressed in the reduced residual Helmholtz function as follows:

$$F^{CPC} = \frac{A^R(T,V,n)}{RT} = m(a^{att} + a^{rep}) + a^{chain} \tag{2.71}$$

where the a^{att} and a^{rep} are given in (2.39) and (2.40), respectively. The a^{chain} is the chain term and expressed by:

$$a^{chain} = -\sum_i n_i(m_i - 1)\,ln[g(\beta)] \tag{2.72}$$

The reduced volume is expressed in (2.62), and the radial distribution function is given by (2.63), which was proposed by Elliott et al.

2.3.6. Applying Equations of State to Polymer Systems

Many researchers started applying cubic equations of state in the past several years, and Sako et al.[37] were the first researchers to apply cubic equations of state to the polymer solutions. Sako developed an equation of state that has three parameters to model the polymer solutions. These parameters are energy (a), co-volume (b), and Prigogine's external degrees of freedom parameter (c) that is associated with polymers. To evaluate the pure component parameters, two adjustable parameters were used to account for the volatility of the fluids and the extension of the polymers. This approach in modeling polymer solutions violates the simplicity of cubic equations of state because of the complexity in evaluating these three parameters for both solvents and polymers. Also, the accuracy of this model was not high comparable with the non-cubic equation of states that requires experimental measurements.

After that, Kontogeorgis, Harismiadis, Fredenslund, and Tassios (KHFT)[38] proposed a new method to calculate the attractive and repulsive parameters for the van der Waals equation of state. Both of a and b parameters of the van der Waals equation were fitted by using two experimental volume-temperature data points at low pressure per polymer. In addition, they used van der Waals one fluid mixing rule to account for polymers mixtures. Two combining rules were used for a_{ij} and b_{ij} along with l_{ij} binary interaction coefficient. These rules were Berthelot and Arithmetic mean combining rules. This model was proved to be better than Flory-Huggins model[38]. It was also proved to be applicable with acceptable results for vapor-liquid equilibrium[39], liquid-liquid equilibrium for polymer solutions[40–42], and Henry constants prediction[43]. However, there is a major

drawback for this model, which is poor prediction of the solution's volume at high pressures. It also gives a huge error for pure polymer vapor pressures, which leads to false results in VLE data for polymers with low molecular weight.[44]

Another contribution is using Peng–Robinson–Stryjek–Vera equation of state (PRSV)[45], which is a modified version of the Peng-Robinson equation of state, in modeling polymer systems. PRSV equation of state proved to have a better accuracy because of using a new term (κ). This new term (κ) is an adjustable pure component parameter that modifies the attraction term in the PR equation of state. Orbey and Sandler (OS)[46] adjusted the equation parameters by fitting them to volumetric data of the pure polymers by assuming the vapor pressure for the targeted polymer is 10^{-7} MPa. However, this method is time consuming since each polymer with different molecular weight will have different parameters. Moreover, this model shows large deviations in the vapor pressures as well as the volumetric behavior when the operating temperatures are high, which will cause a bad prediction for the VLE in polymer solutions.[44] Wong and Sandler[47] presented a new mixing rule to correlate this poor prediction of the VLE data. This mixing rule depends on two binary interaction parameters. Then, Zhong and Masuoka[48] adjusted Wong and Sandler mixing rules by reducing the binary interaction parameters to only one parameter by setting the excess Helmholtz energy at infinite pressure to zero.

Moreover, there are many other researchers who tried to improve the correlation and prediction of the polymer phase behavior either by adjusting the available equations of states parameters or changing the mixing rules. As mentioned earlier in this chapter, Gross and Sadowski proposed a modified version of the SAFT equation which is

perturbed-chain SAFT (PC-SAFT) equation of state. This equation showed good results in modeling the VLE, LLE, and VLLE for binary and ternary mixtures of polymers, gases, and solvents.[21] Gross and Sadowski compared both of SAFT and PC-SAFT to model different polymer systems, and PC-SAFT was proven to have better accuracy than SAFT equation. Both models considered to be more complex and time-consuming than cubic equations of state.[4]

Chapter 3

Modeling Polymer Systems Using Cubic-Plus-Chain (CPC) Equation of State

3.1. Introduction

Understanding the phase equilibrium behavior of polymers attracts the interest of the researchers and the petrochemical industries since polymer represents a crucial factor in these industries. Investigating different types of polymers as well as their solvents is necessary for having successful industrial plants. Knowing these concepts and how to apply them for polymer processes is an important tool to learn since many polymers are processed as solutions. Phase equilibrium behavior for polymer solutions is an essential concept to learn because of its applicability in polymeric membrane separation processes, polymer devolatilization, paints, coatings, gels that are used in hydraulic fracturing, or even producing light-emitting devices.[49]

Solvents selection plays an important role in polymer processing. If wrong solvents were chosen, they could lead to a deposition of the polymer in the reactor, flash drums, heat exchangers, or even clog the process pipelines.[50] Therefore, the solubility as well as the phase behavior of these polymers with the solvents need to be investigated whether it is vapor-liquid equilibrium (VLE), liquid-liquid equilibrium (LLE), or solid-liquid

equilibrium (SLE) in order to prevent these problems. Modeling these cases is crucial in understanding the behavior of these polymer-solvent systems since many empirical models cannot describe these complex systems.

In this chapter, different polymer systems are modeled with different solvents with using the CPC equation as well as the PC-SAFT equation of state. These polymer-solvent systems involve polypropylene, polyethylene, and polystyrene systems. Both CPC and PC-SAFT modeling results are compared with experimental data from the literature. The effect of molecular weight, concentration, temperatures, solvent selections, and polydispersity on the phase behavior modeling are studied. In addition, the binary interaction parameter (k_{ij}) for CPC is investigated for polymer systems as well as 15 well defined systems in order to study the factors that affect the k_{ij}.

3.2. Modeling Technique

The phase equilibrium conditions and constraints that were mentioned in Chapter 2 need to be used in order to study the phase behavior for different polymer-solvent mixtures efficiently. For polymer-solvent systems, vapor-liquid and liquid-liquid phase equilibria are encountered; therefore, the partition functions that relates both of those phases are given by:

$$K_i = \frac{y_i^v}{y_i^l} = \frac{\hat{f}_i^v}{\hat{f}_i^l} \frac{\hat{\phi}_i^l}{\hat{\phi}_i^v} \frac{P}{P} = \frac{\hat{\phi}_i^l}{\hat{\phi}_i^v} \tag{3.1}$$

$$K_i = \frac{y_i^{l_1}}{y_i^{l_2}} = \frac{\hat{f}_i^{l_1}}{\hat{f}_i^{l_2}} \frac{\hat{\phi}_i^{l_2}}{\hat{\phi}_i^{l_1}} \frac{P}{P} = \frac{\hat{\phi}_i^{l_2}}{\hat{\phi}_i^{l_1}} \tag{3.2}$$

Where v, l_1, and l_2 account for the vapor, liquid 1, and liquid 2 phases, respectively. If the partition coefficient in equation (3.1) is greater than zero, it means that there are more concentrations of component i in v phase than l phase because the partition function works as a tendency indicator for the species to favor one phase over the other. Similar argument can be stated for equation (3.2).

Cubic-plus-chain (CPC) is a new equation of state, and it was not applied intensively for polymer systems; therefore, the pure component parameters for polymer were not available. Hence, it is crucial to find those parameters in order to model the phase equilibrium behavior accurately. There are two approaches that were studied in determining the pure component parameters for polymers. The first approach was tuning the monomer chain length (m_{mono}) to match saturation pressure and density. After that, the monomer chain lengths along with the critical temperature (T_c) and critical pressure (P_c) are used to calculate a_i and b_i in the CPC equation. Then, the number of monomer segments in the polymer (m_{poly}) is tuned to binary phase equilibrium data to account for the total chain length of the polymer as shown in equation (3.3). For instance, polyethylene can be modeled using the pure component parameter for ethane to calculate a and b parameters. This approach worked for a few systems and failed to model many other systems because of different reasons. The shielding effect and entanglement could not be taken in consideration properly when this approach was used.[21] Molecular effects limit the use of this approach. Therefore, another approach needs to be proposed to model the polymer systems. In this new approach, the experimental cloud points for different binary mixtures at different temperatures need to be used to accurately tune the CPC parameters. Three parameters were tuned for each

polymer, and these parameters are Ω_A, Ω_B, and m_{poly}/M_w. Those Ω_A and Ω_B were used to calculate both of a and b pure-component parameters in CPC, which involved using T_c and P_c values for the reference monomer by equations (2.35) and (2.36). The polymer chain length in the CPC equation is defined as follows:

$$m = m_{mono}m_{poly} \tag{3.3}$$

Where m_{mono} and m_{poly} are the chain length of the reference monomer and the number of monomer segments in the polymer, respectively. The tuned m_{mono} and m_{poly} are used to account for the total length of the polymer (m). The reference monomer is ethane for polyethylene, propane for polypropylene, and styrene for polystyrene. This approach shows an excellent phase behavior modeling in comparison with experimental cloud points for all of the systems that are mentioned in this chapter. The pure component parameters by using this approach for different polymers are given in **Table 3.1**.

Table 3.1. Pure-Component Parameters of the CPC Equation of State for Polymers

Systems	Ω_A [−]	Ω_B [−]	m_{mono} [−]	m_{poly}/M_w [mol/g]
Polypropylene	0.177	0.046	1.7047	0.012
HDPE	0.425	0.060	1.3301	0.0165
LDPE	0.420	0.060	1.3301	0.0165
Polystyrene	0.411	0.067	3.3500	0.0075

3.3. Modeling Polymer Phase Behavior

3.3.1. Polypropylene Systems

Polypropylene (PP) was discovered in 1951 by two chemists, who are Hogan and Banks[3], by polymerizing propylene. Polypropylene is a thermoplastic polymer since it is moldable and pliable at high temperature. It can be used for many various industrial, households, and medical purposes.[51] It is fatigue resistance because it can retain the original shape after applying a load to it. It also can be used in electronic devices and automobiles since it has a high electric resistance. Polypropylene can be used to make containers since it does not react at room temperature with many organic solvents. Polypropylene can copolymerize with other polymers such as polyethylene to be engineered for different applications since the copolymerization changes the pure polymer properties.

Polypropylene can be produced by chain polymerization of propylene with using catalysts. Chain polymerization is a mechanism where the monomer is added to the end parts of a growing chain since they considered to be the active sites of the chain. The propylene and polypropylene chemical structures are shown in the following figure.
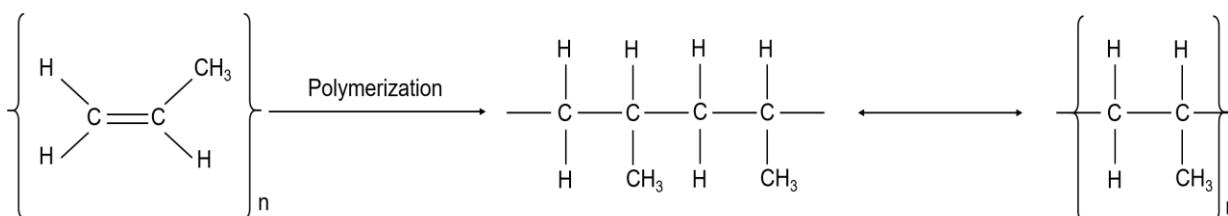

Figure 3.3.1. Chemical structures for both Propylene and Polypropylene.

The chemical structure in **Figure 3.3.1** depicts the polymerization process of propylene to form polypropylene. The double bond in the propylene consists of two bonds, namely σ and π bonds. When the polymerization process occurs, π bonds are destroyed since they are weaker than σ bonds in propylene molecules.

The first system is a mixture of Polypropylene-n-Pentane system. This system is modeled using three different temperatures ranging from 177 ℃ to 197 ℃. The system was modeled with the CPC equation mentioned in Chapter 2; however, the parameters were not available for this system. Therefore, Ω_A, Ω_B, m_{poly}/M_w, and k_{ij} were tuned for the polypropylene to match the experimental cloud-point pressure data given by Martin et al[52]. These parameters are shown in **Table 3.1**. The same approach was done by Gross and Sadowski[21] for identifying the pure component parameters for different polymers. The polypropylene in this system is modeled as a monodisperse polymer since the ratio of weight-average molecular weight (M_w) to the number-average molecular weight (M_n) is 2.2.[52] The CPC modeling results for this system are compared with PC-SAFT equation of state in

Figure 3.3.2. The regular cubic equations of state could not predict the polymer-solvent mixtures. Moreover, Gross and Sadowski proves that the PC-SAFT equation of state shows a better prediction of the phase behavior than the SAFT equation of state.[21] Hence, it was not necessary to compare cubic and SAFT equations of state to CPC equation of state in this chapter.
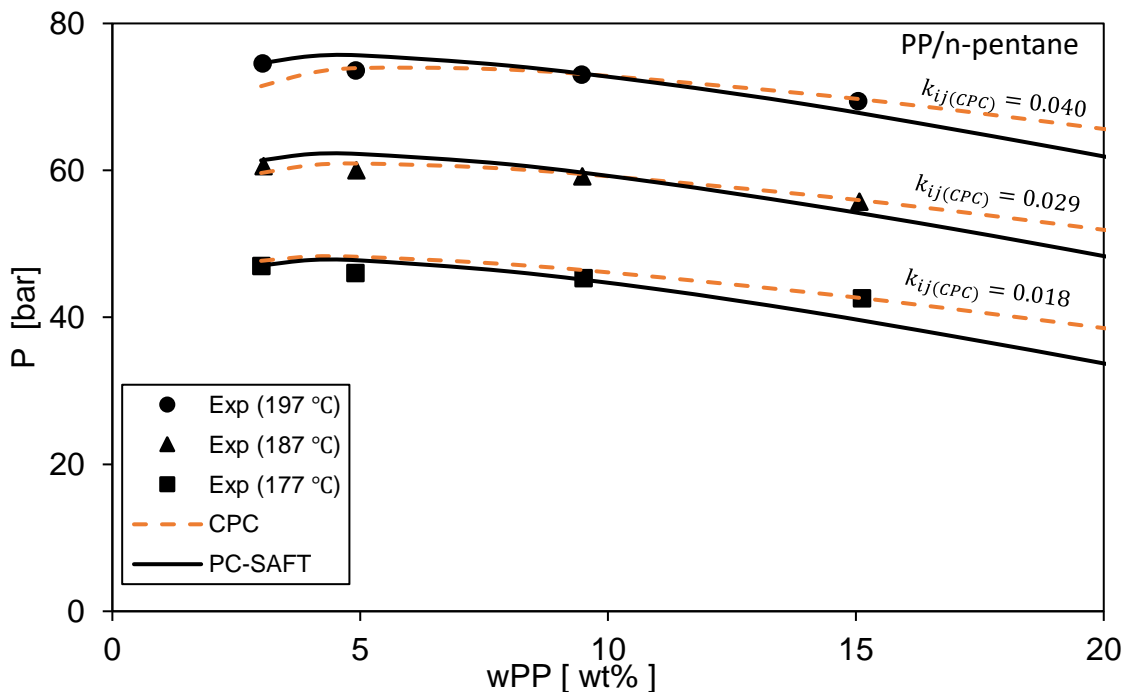
Figure 3.3.2. Liquid-liquid equilibrium (LLE) of Polypropylene-n-Pentane at three different temperatures (PP: M_W = 50.4 kg/mol). Comparison of both CPC using three different k_{ij} and PC-SAFT ($k_{ij} = 0.0137$) with experimental cloud points[52].

Both of the CPC equation and the PC-SAFT equations of state show an excellent prediction comparing to experimental phase behavior data. The CPC equation shows a similar prediction of the cloud-point pressures modeled with PC-SAFT equation. Three different binary interaction parameters were used to model this system with CPC, and the values for this parameter is 0.018, 0.029, and 0.040 for 177 °C, 187 °C, and 197 °C, respectively. A linear equation relating binary interaction parameter to temperature for this system is proposed and shown in Appendix B. On the other hand, only one constant binary interaction value was used for modeling PC-SAFT equation for different temperatures. Using a temperature dependence k_{ij} in CPC could be because of the lack of the temperature dependent parameter in the excluded volume (B). In addition, the radial distribution function in CPC is temperature-independent whereas the PC-SAFT equation

uses a temperature-dependent radial distribution function with a temperature dependence term in the monomer segment diameter.

Another example is modeling a mixture of polypropylene and propane at three different temperatures. The polypropylene in this system is assumed to be polydisperse with a molecular weight distribution of three pseudo-components because the ratio of M_w to M_n is 4.4.[53] A comparison of CPC with PC-SAFT equations of state is modeled and shown in **Figure 3.3.3** for three different temperatures.
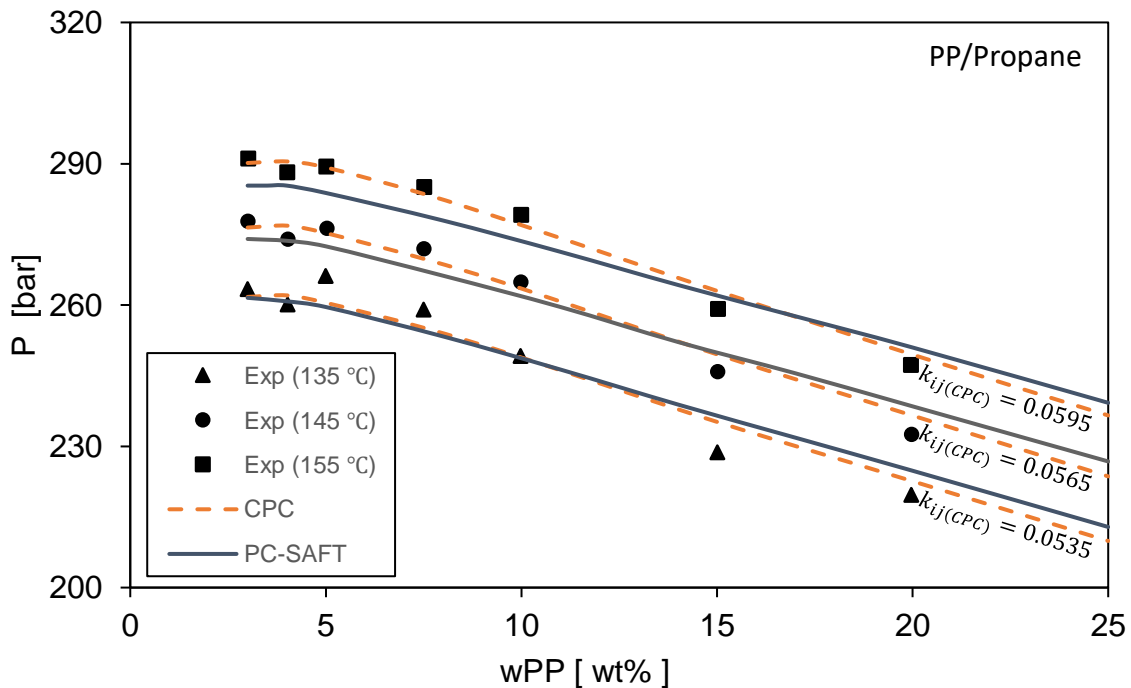
Figure 3.3.3. Liquid-liquid equilibrium (LLE) of Polypropylene-Propane at three different temperatures (PP: M_W = 290 kg/mol). Comparison of both CPC using three different k_{ij} and PC-SAFT ($k_{ij} = 0.0242$) with experimental cloud points[53].

Figure 3.3.3 illustrates how good the prediction of both equations of state with the experimental could points given by Whalet et al.[53] for three different temperatures. The CPC model shows a similar correlation in comparison with the PC-SAFT equation for this

system. It is crucial to use the same tuned Ω_A, Ω_B, and m_{poly}/M_w values for polypropylene except the binary interaction parameter needed to be changed in order to better match the experimental data for Polypropylene-Propane mixture. This is an indication that the CPC equation of state is applicable in modeling polypropylene systems. Again, the use of binary interaction parameter is because of the failure of the equation of state to model the mixtures because of using an inadequate mixing rule. CPC require using three different binary interaction values for three different temperatures; however, only one binary interaction value is required to be used in the PC-SAFT equation.

The effect of polydispersity is studied for this binary system. In the following figure, polypropylene was modeled by considering it a monodisperse and compare it with the previous result when PP was modeled to be polydisperse.
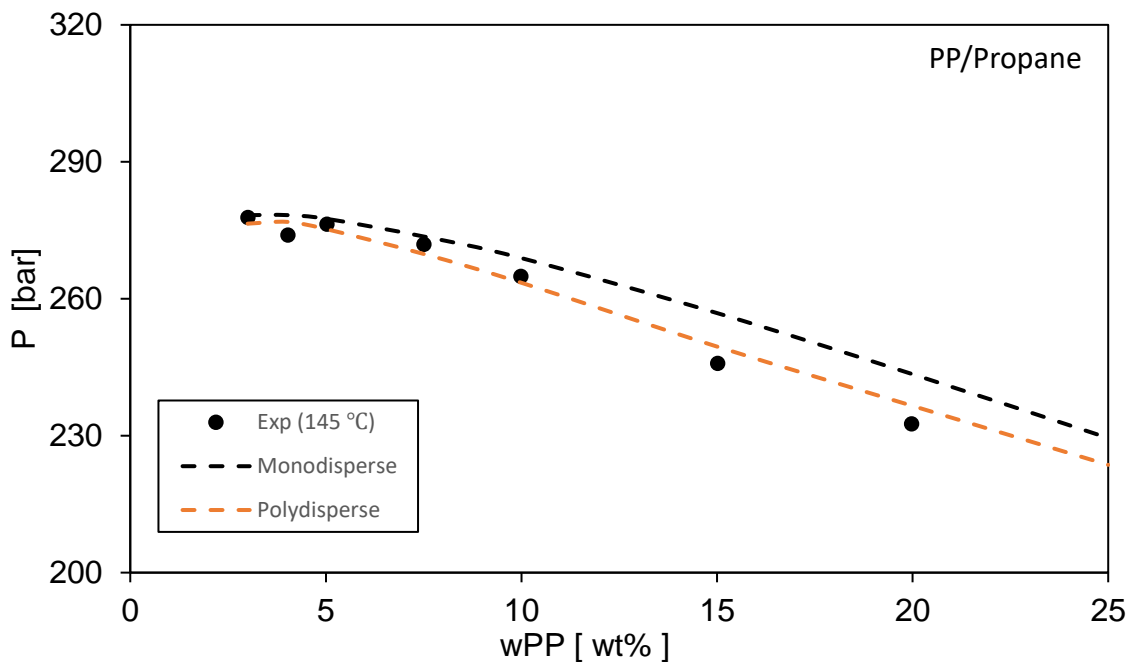

Figure 3.3.4. Liquid-liquid equilibrium (LLE) of Polypropylene-Propane at 145 °C (PP: M_W = 290 kg/mol). Comparison of modeling PP as monodisperse and polydisperse using CPC ($k_{ij} = 0.0565$) with experimental cloud points[53].

Figure 3.3.4 depicts how good the CPC model in predicting the phase behavior when the polymer is modeled as polydisperse consisting of three pseudo-components at a given weight percent range. However, it shows a small deviation if this polymer is modeled as a monodisperse and the parameters are kept constant. The monodisperse polymer would show a better cloud-point pressures for the given polymer weight percent range if the binary interaction parameter is set to be 0.0550 instead of 0.0565.

3.3.2. Polyethylene Systems

Polyethylene (PE) is the most common plastic considered to produce approximately one-third of plastic worldwide.[54] Polyethylene was discovered in 1898 by Hans von Pechmann[55] while he was preparing diazomethane. It can be copolymerized with different monomers to produce new compounds with enhanced properties. There are different types of polyethylene, and they are mainly categorized based on branching and density.[2] High-density polyethylene (HDPE) and low-density polyethylene (LDPE) will be investigated in this chapter with different solvents. Both of these polymer's category has its own properties. HDPE has less hydrocarbon branching than LDPE, which makes the intermolecular forces of HDPE to be higher than LDPE. The lower the branching leads to having a higher surface area that results to an increase in the intermolecular forces. LDPE is widely used in making plastic bags and containers; however, HDPE can be used in pipes manufacturing as well as detergent bottles.[2] Polyethylene is a result of polymerization of ethylene upon contacting with catalysts. The following figure depicts both of ethylene and polyethylene chemical structures.
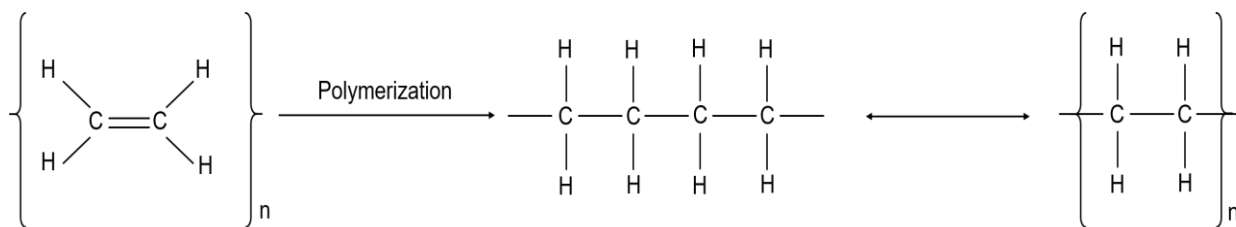
Figure 3.3.5. Chemical structures for both Ethylene and Polyethylene.

Both of HDPE and LDPE were modeled with different solvents to study the phase behavior equilibrium by using CPC equation of state and compare it with the PC-SAFT equation of state. Gross and Sadowski modeled these systems with PC-SAFT and compare it with SAFT. Their comparison proves that PC-SAFT predicts cloud-point pressure better than the SAFT equation. Hence, the CPC equation will be compared with the PC-SAFT equation in this work for different polyethylene-solvent systems. HDPE-ethylene mixture is modeled in **Figure 4.5** by considering it to be monodisperse in terms of molecular weight distribution for HDPE with a ratio of M_w to M_n of 2.7.[56] The pure component parameters for the CPC model are shown in **Table 3.1**, and the pure component parameters for the PC-SAFT model are shown in Appendix B.
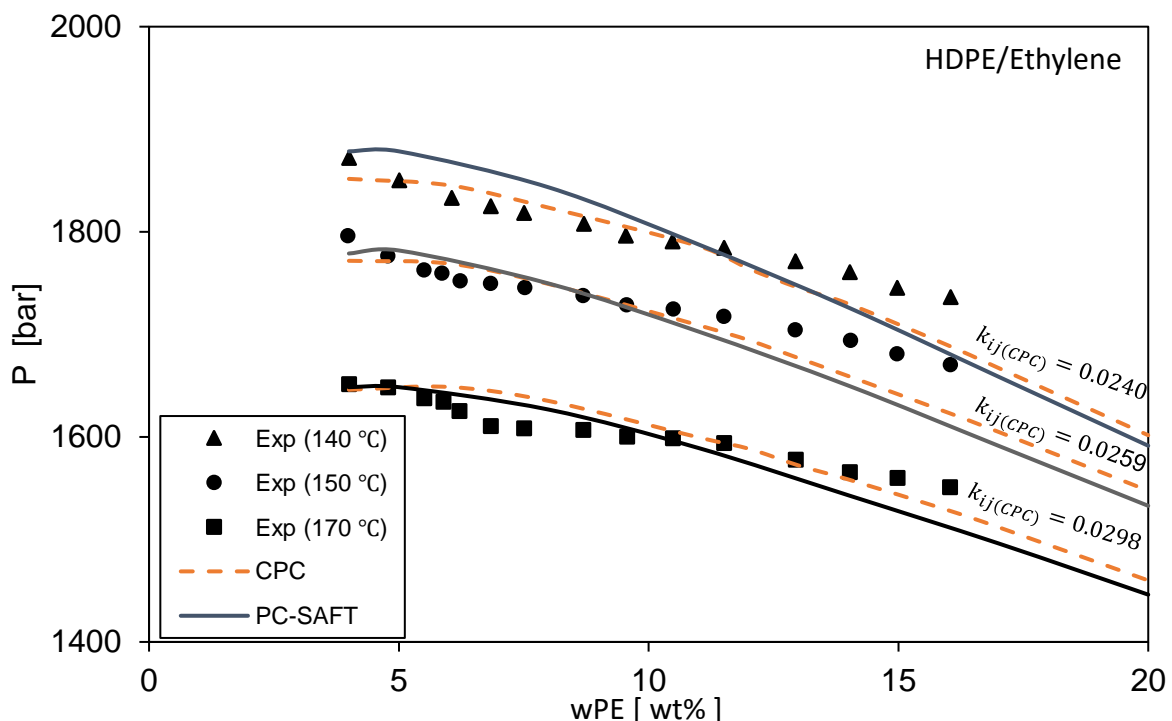
Figure 3.3.6. Liquid-liquid equilibrium of High-Density Polyethylene (HDPE)-Ethylene at three different temperatures (HDPE: M_W = 118 kg/mol). Comparison of both CPC using three different k_{ij} and PC-SAFT ($k_{ij} = 0.0404$) with experimental cloud points[56].

This figure illustrates the efficiency of modeling cloud-points pressure in terms of weight fraction of the polymer at three different temperatures. CPC is compared with PC-SAFT in modeling HDPE-ethylene mixture, and the CPC model shows a similar representation of the experimental cloud points in comparison with the PC-SAFT modeling results. However, the CPC equation requires using temperature dependence binary interaction parameter whereas PC-SAFT uses a constant binary interaction parameter.

HDPE-ethylene system involves using a high-pressure reactor as well as flash units. After this process, there will be some amount of ethylene left in the polyethylene. This system at high polyethylene weight amount ranging from 95% to 100% with ethylene is modeled in **Figure 3.3.7** with two different temperatures.
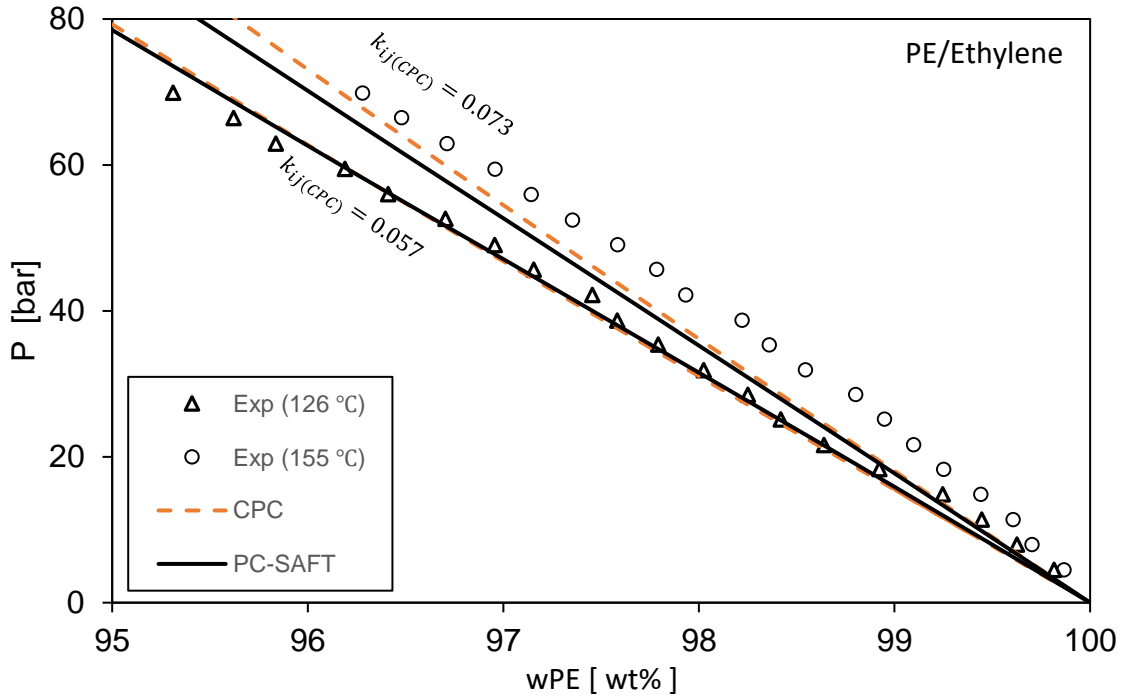
Figure 3.3.7. Vapor-liquid equilibrium of Polyethylene (HDPE)-Ethylene at two different temperatures (PE: M_W= 248 kg/mol). Comparison of both CPC using two different k_{ij} and PC-SAFT ($k_{ij} = 0.0404$) with experimental cloud points[57].

This figure shows the vapor-liquid equilibrium of polyethylene (PE) and ethylene mixture at two temperatures by using the same parameters used in **Figure 3.3.6.** The parameters Ω_A, Ω_B, and m_{poly}/M_w for the CPC equation that are required to use in this system are the same for HDPE-ethylene system even though the molecular weight is different. In addition, this figure is an indication for the applicability of extrapolation by using the same initial parameters across different weight fractions and temperatures as long as k_{ij} is tuned to match the cloud-point pressures. Again, using the CPC equation in modeling this system shows a similar prediction as the PC-SAFT results. However, the k_{ij} for PC-SAFT is constant for both of **Figure 3.3.6.** and **Figure 3.3.7**.

Another example of modeling HDPE with different solvent by using the CPC equation is studied to investigate the effect of choosing different solvent on the prediction of the cloud-point pressure. A mixture of HDPE-n-Pentane is modeled in the following figure and compared to experimental cloud points. HDPE in this modeling was considered to be monodisperse.
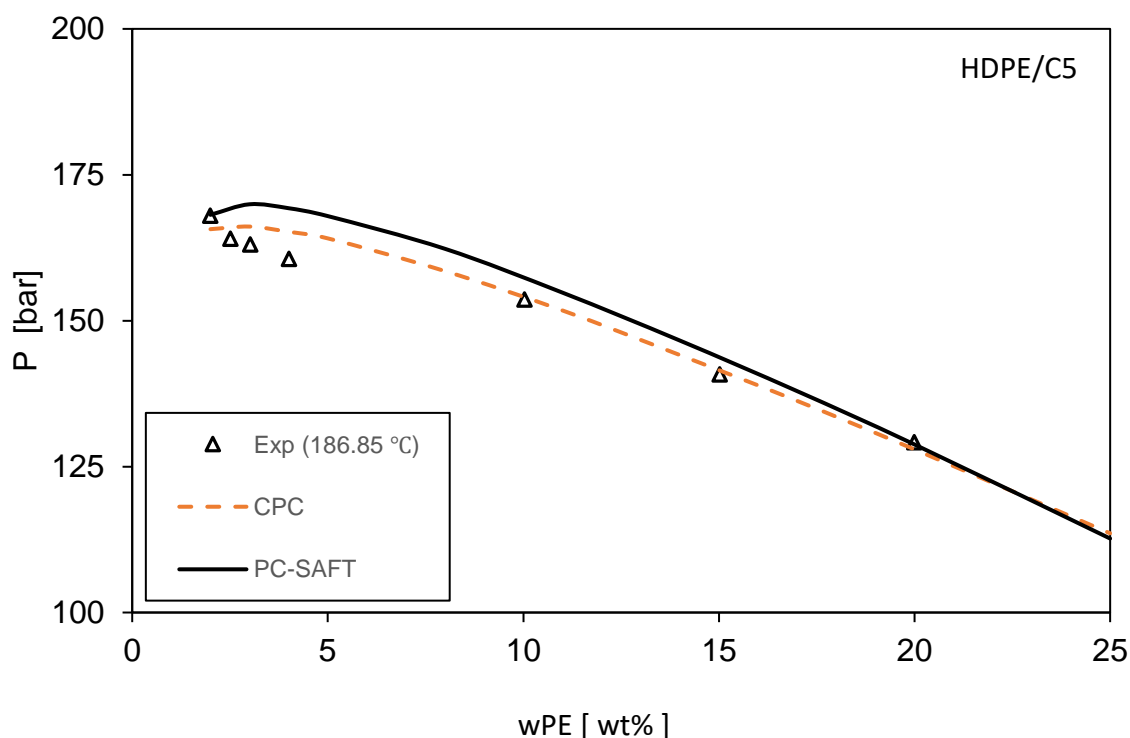
Figure 3.3.8. Liquid-liquid equilibrium of High-Density Polyethylene (HDPE)-n-Pentane at $T = 187\ °C$ (HDPE: M_W= 121 kg/mol). Comparison of both CPC ($k_{ij} = -0.049$) and PC-SAFT ($k_{ij} = 0.000$) with experimental cloud points[58].

In this figure, the liquid-liquid equilibrium of HDPE and n-pentane binary mixture is modeled with two different equations of state in order to study their accuracy in predicting cloud-point pressure in comparison with experimental cloud points. The CPC model uses the same pure component parameters that were obtained for HDPE; however, the binary interaction parameter needs to be adjusted since different

temperature and solvent are being used in this mixture. The CPC model with these pure component parameters and a binary interaction parameter value of -0.049 shows a similar prediction to PC-SAFT result with using k_{ij} value of 0. The reason that a negative k_{ij} is used in CPC is because the model overpredicts the cloud-point pressure. Using a negative k_{ij} value reduces the overprediction because of its effect on calculating the molecular interaction energy parameter (A), which will be explained intensively in this chapter.

Another example of using an aromatic solvent with different molecular weights of polyethylene is investigated. Two different molecular weights of PE with toluene solvent is illustrated in **Figure 3.3.9** to study the applicability of using the CPC equation when the solvent and the molecular weight are different. The same pure component parameters, which are Ω_A, Ω_B, and m_{poly}/M_w, for HDPE are being used for polyethylene with two different molecular weight values of 1710 and 6220 g/mol. Both of Ω_A and Ω_B are used to calculate a and b pure-component parameters in the CPC equation.
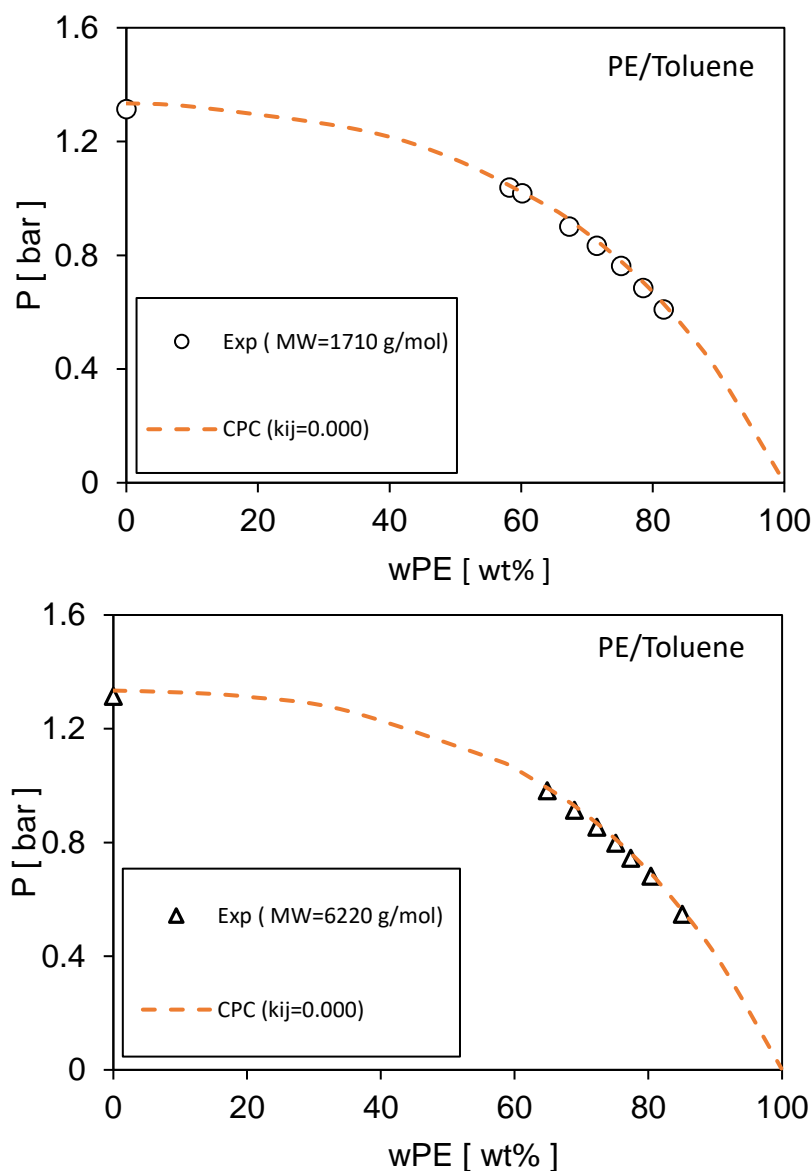
Figure 3.3.9. Vapor-liquid equilibrium of Polyethylene (HDPE)-Toluene at $T = 120\ °C$ for two different molecular weight values. Comparison of CPC ($k_{ij} = 0.000$) with experimental cloud points [59].

The saturation pressure at vapor-liquid equilibrium for PE-toluene mixture is shown in

Figure 3.3.9 by using the CPC equation of state. The binary interaction parameter k_{ij} in

this mixture was set to be zero for both of molecular weight. Since the model shows a

perfect prediction to the experimental data, it means that the CPC model works perfect

for saturation pressure prediction for this binary system. The pure component parameters for this system is shown in **Table 3.1**.

Another type of polyethylene is LDPE, which is known as low-density polyethylene. The phase behavior of a mixture of LDPE with ethylene is investigated for three different temperatures. The LDPE was modeled using six pseudo-components with M_w/M_n value of 8.56 [60]. The following figure shows a comparison between the prediction of cloud-point pressures for this binary mixture by using CPC and PC-SAFT equation of state.

Figure 3.3.10. Liquid-liquid equilibrium of Low-Density Polyethylene (LDPE)-Ethylene three different temperatures (LDPE: M_W= 165 kg/mol). Comparison of both CPC using three different k_{ij} values and PC-SAFT ($k_{ij} = 0.039$) with experimental cloud points[60].

In this figure, liquid-liquid equilibrium for a mixture of LDPE-ethylene at three different temperatures is modeled by using the CPC and PC-SAFT equations. Similarly, the pure component parameters were obtained following the same approach used for the

previous systems. The parameters Ω_A, Ω_B, and m_{poly}/M_w in the CPC model were tuned to match the cloud-point data, and these parameters are shown in **Table 3.1**. However, the binary interaction parameter was tuned for three different temperatures. The pure component parameters for the PC-SAFT model were available in the literature for LDPE and provided in Appendix B. The values of six pseudo-components for LDPE are shown in the same Appendix. A linear equation that relates the binary interaction parameter to the temperature in order to extrapolate the values away from this temperature range is also shown in the same Appendix.

In the following figure, LDPE was modeled by considering it a monodisperse and compare it with the previous result when LDPE was modeled to be polydisperse.
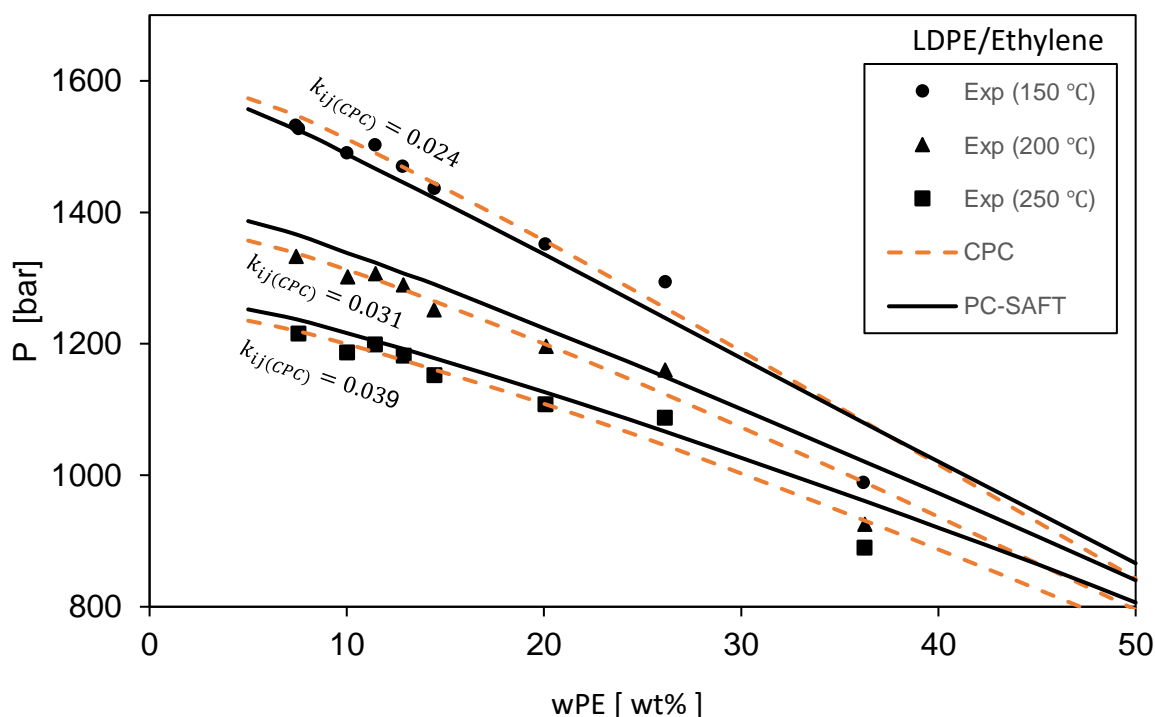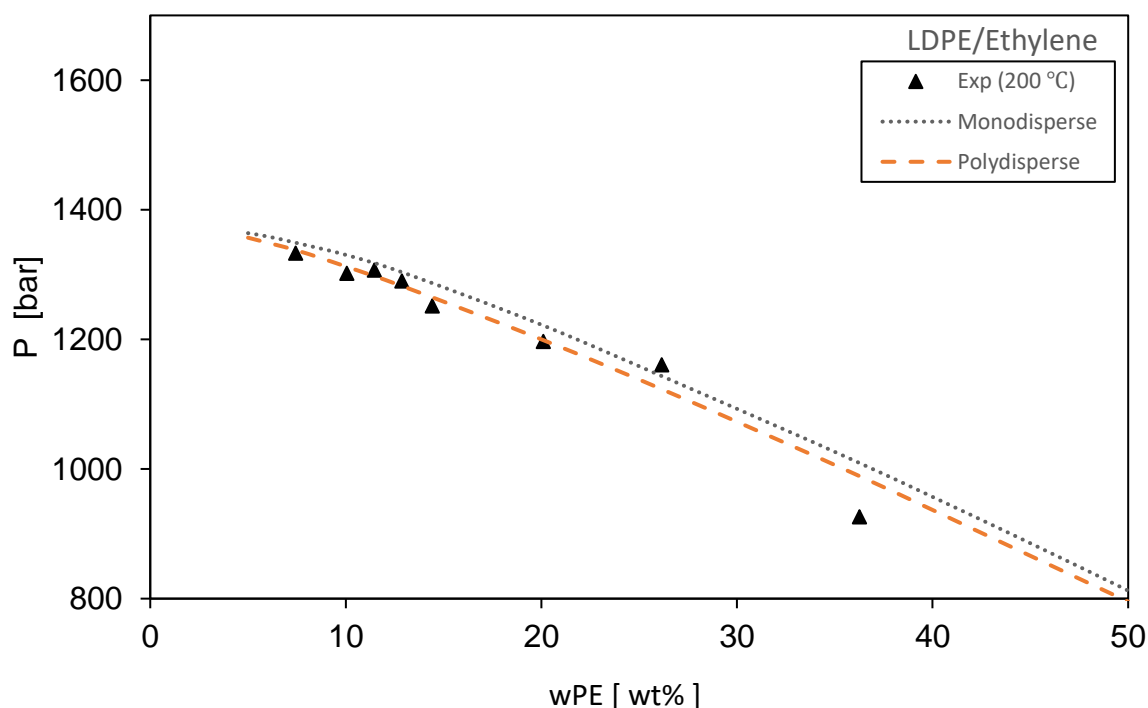

Figure 3.3.11. Liquid-liquid equilibrium of Low-Density Polyethylene (LDPE)-Ethylene at 200 °C (LDPE: M_W= 165 kg/mol). Comparison of modeling LDPE as monodisperse and polydisperse using the CPC model ($k_{ij} = 0.031$) with experimental cloud points[60].

In **Figure 3.3.11**, the CPC model shows that it can be used to predict the phase behavior of polydisperse LDPE of six pseudo-components with ethylene solvent properly. However, if LDPE was modeled to be monodisperse with keeping all of the parameters to be constant, it overpredicts the cloud-point pressures. This problem can be solved by adjusting the binary interaction parameter to lower down pressure predictions since the model shows a correct shape with a shifted trend. This example as well as previous examples prove that CPC works for polymer-solvent systems at given polymer concentration ranges despite changing the polymer type, polydispersity, molecular weight, temperature, or even polymer concentration.

3.3.3. Polystyrene Systems

Polystyrene (PS) is a chain of hydrocarbon consisting of alternating carbon centers that are bonded to a phenyl group. It was first discovered by Eduard Simon[61] in 1839. Polystyrene is a colorless material with a limited flexibility; however, it can be colored to different colors depends on the targeted purposes and application. [62] Polystyrene is used for manufacturing smoke detectors, frames, plastic model tools, and foams. It can be copolymerized with different monomers to create a new material with different properties. There are three different polystyrene classes. These categories are polystyrene foam, plastic, and film.

Polystyrene can be polymerized by using free radical polymerization of styrene monomer. Styrene has a double bond in the vinyl group consisting of a weak bond (π) and a stronger bond (σ). In the polymerization process, the weak bond breaks and a new stronger bond (σ) forms with adjacent carbon atom from different styrene monomer.

Since the new bond that is formed in the polymerization process is stronger; hence, it is hard to depolymerize and break this bond. The chemical structure for styrene as well as the polystyrene is shown in the following figure.
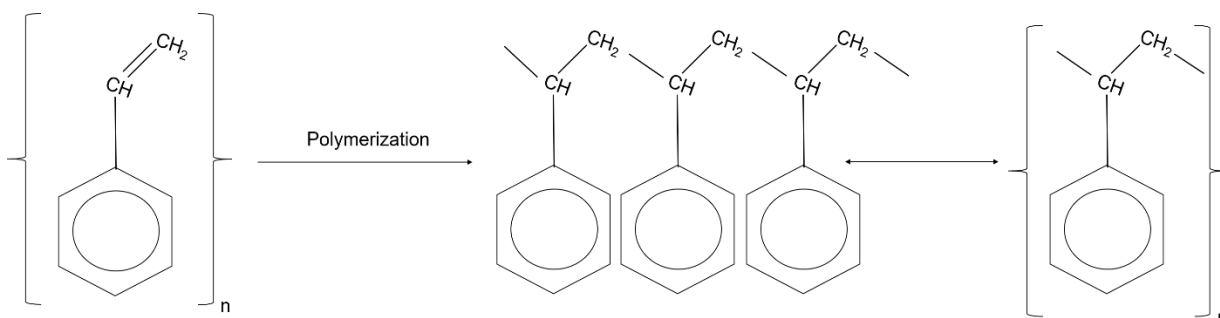
Figure 3.3.12. Chemical structures for both Styrene and Polystyrene.

Phase behavior of a binary mixture of polystyrene and ethylbenzene is investigated. A vapor-liquid equilibrium (VLE) of this mixture is modeled at two different temperatures using two equations of state, namely the CPC and the PC-SAFT equations. Both models show a good correlation to the experimental saturation pressure data using binary interaction parameter value of zero in both models, and the polymer is considered to be monodisperse. The vapor-liquid equilibrium for this system is shown in **Figure 3.3.13**.
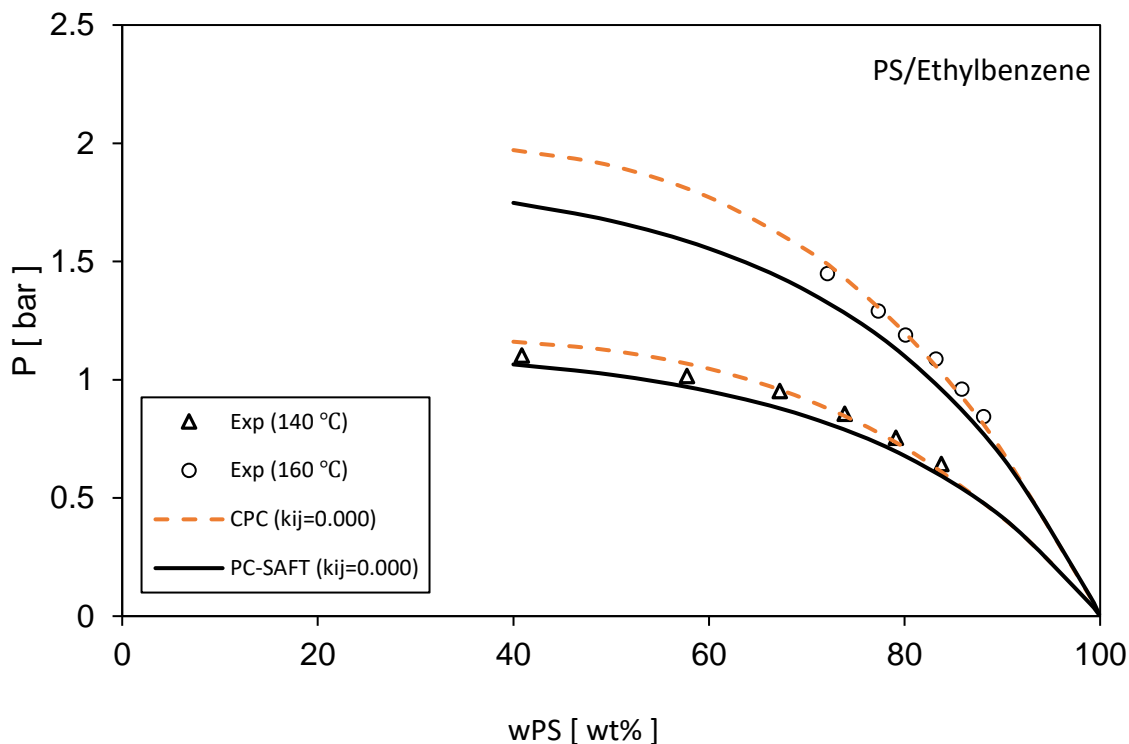
Figure 3.3.13. Vapor-liquid equilibrium of Polystyrene (PS)-Ethylbenzene at 140 °C and 160 °C (PS: M_W = 93 kg/mol). Comparison of both the CPC and the PC-SAFT models with experimental cloud points[63] .

Figure 3.3.13 shows the phase behavior of polystyrene and ethylbenzene at two different temperature. The pure component parameters for PS were obtained following the same approach used for the previous systems. The parameters Ω_A, Ω_B, and m_{poly}/M_w in the CPC model were tuned to match experimental cloud-point pressures, and these parameters are shown in **Table 3.1**. The CPC equation proved to model vapor-liquid equilibrium for PS-ethylbenzene system with using a zero k_{ij} value for two different temperatures. Also, the PC-SAFT equation was used in modeling this system. The modeling results of the CPC equation are compared with both the PC-SAFT equation and experimental cloud points. The PC-SAFT equation would match the experimental cloud-point pressures if the binary interaction parameter is changed.

3.4. Sensitivity Analysis

A sensitivity analysis is a study that shows the uncertainty of the modeling result if the input parameters of a mathematical model are changed. It is a tool that is used to analyze the impact of different independent variables on a specific dependent variable. Hence, a sensitivity analysis is used in determining which factor affects the modeling results of the CPC equation the most. A binary mixture of polypropylene-propane is used to identify the impact of each parameter in the CPC equation on the cloud-point pressures. The sensitivity analysis method is used by changing each of $\Omega_A, \Omega_B, m_{poly}/M_w$, and k_{ij} one at a time by $\pm 2.5\%$ and $\pm 5\%$. The sensitivity analysis of those four parameters were analyzed by the absolute percentage deviation from the experimental values as follows:

$$\% \text{ AAD}_X = \frac{\left|X^{model} - X^{exp}\right|}{X^{exp}} \times 100 \tag{3.4}$$

Where X^{exp} and X^{model} are the output experimental value and model output value based on the parameter modification, respectively. A sensitivity analysis is performed for a polydisperse polypropylene with propane mixture as shown in **Figure 3.4.1**.
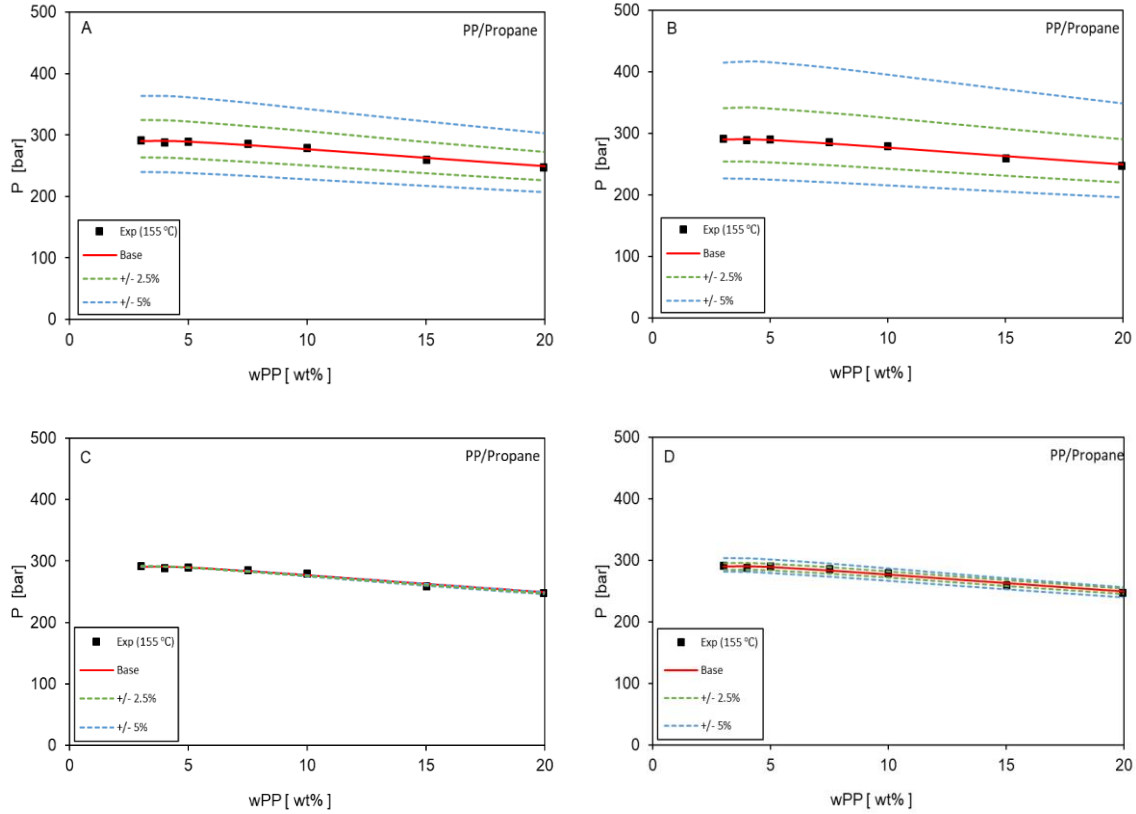
Figure 3.4.1. Sensitivity analysis of CPC parameters **(A)** Ω_A, **(B)** Ω_B, **(C)** m_{poly}/M_w, and **(D)** k_{ij} for polypropylene-propane mixture at T= 155 °C with experimental cloud points[53].

Figure 3.4.1 represents the sensitivity analysis of four parameters, which are

$\Omega_A, \Omega_B, m_{poly}/M_w$, and k_{ij}. These parameters were changed one at a time by $\pm$ 2.5% and

$\pm 5\%$ with respect to the base values that can be found in **Table 3.1**. According to the

figure above, Ω_B coefficient shows to have the highest impact on the modeling result in

comparison with the other parameters since this coefficient is used in calculating

excluded volume parameter (b_i) that is used in the attractive, repulsive, and chain terms

in the CPC equation of state. The coefficient Ω_A shows to have the second highest impact

in terms of sensitivity in modeling polymer-solvent systems. Again, Ω_A is used in

calculating the interaction energy parameter (a_i) in the CPC equation. Both of Ω_A and Ω_B

shows to be very sensitive because if wrong values were assigned for those parameters,

they would not represent the correct volume and interaction energy of the specific polymer. The true values for Ω_A and Ω_B are crucial to have in modeling polymer systems, and those values are presented in **Table 3.1** for different polymer systems. The binary interaction parameter shows to be less sensitive than Ω_A and Ω_B when the temperature is constant; however, it is more sensitive than m_{poly}/M_w. The reason of this sensitivity is because k_{ij} is used in calculating the mixing rule of the interaction energy parameter, and the value of k_{ij} used in this mixture is very small. Hence, it did not affect the interaction energy parameter for the mixture (A) significantly. The parameter m_{poly}/M_w shows to have the least impact on the model sensitivity analysis since the value is very small. In addition, the change to this parameter propagates through the numerator and the denominator of the CPC equation of state since this change affects the mixing rules and the chain term of the CPC equation. The absolute percentage deviation from the experimental values for all of the four parameters were analyzed by using equation (3.4). The average absolute deviation values with reference to experimental data are presented in **Table 3.2**.

Table 3.2. Average Absolute Percentage Deviation Based on Sensitivity Analysis of CPC Parameters

Parameters	-5%	-2.5%	Base	$+2.5\%$	$+5.0\%$
Ω_A	16.98	9.079	0.5299	11.27	24.56
Ω_B	42.51	17.39	0.5299	12.24	21.67
$\dfrac{m_{poly}}{M_w}$	0.6509	0.5977	0.5299	0.6079	0.6795
k_{ij}	3.119	1.528	0.5299	2.099	4.091

Table 3.2 illustrates the average percentage error in comparison with experimental data. The base model shows to have the least error. If the parameters of this base model are altered by $\pm2.5\%$ and $\pm5.0\%$, it shows that both of Ω_A and Ω_B are very sensitive with respect to this change. The coefficient Ω_B proved to have the highest impact in terms of sensitivity based on alteration of $-5\%, -2.5$, and $+2.5\%$. However, Ω_A shows to more slightly more sensitive than Ω_B when the 5.0% deviation is considered. Therefore, Ω_B proved to have the highest overall effect to the modeling results followed by Ω_A, k_{ij}, and m_{poly}/M_w, respectively.

3.5. Binary Interaction Parameter for the CPC Equation of State

Binary interaction parameter (k_{ij}) is a parameter that is used to correct the deviation between the experimental data and the equation of state's modeling data for a mixture of component i and j. It represents the deficiency in capturing the intermolecular forces

between the components in binary systems. The use of the binary interaction parameter is a result of an inadequate prediction of the equation of state because of using inappropriate mixing and combining rules for the targeted system. The equation of state could describe the pure component but when it is applied to a mixture, it shows a deviation from the experimental data so that a binary interaction is used to adjust the model's prediction in order to match or get very close to the experimental data. When the binary interaction parameter is zero or very close to zero, it means that the model describes the intermolecular interactions efficiently. The values for binary interaction parameters can be positive or negative depends whether the model is underpredicting or overpredicting the real behavior. For example, if the k_{ij} value that needs to be used is positive, it means that the model with zero k_{ij} value overpredicts the molecular interaction. When the needed k_{ij} value is negative, it means the model underpredict the molecular interaction.

Binary interaction parameter in the CPC model shows to be temperature dependent in modeling polymer systems as shown earlier in this chapter. However, this parameter needs to be investigated for some well-defined systems in order to determine the factor that affects the CPC modeling the most. The CPC equation is a new equation of state that does not have a data set for binary interaction parameters for different systems. Hence, 15 well-defined systems are studied in this chapter to confirm the dependency of k_{ij} with temperature as observed with polymer systems.

Starting with methane-propane system, the binary interaction parameter for three different temperatures was investigated. The following graph shows how the binary interaction changes for changing the temperature for this system.
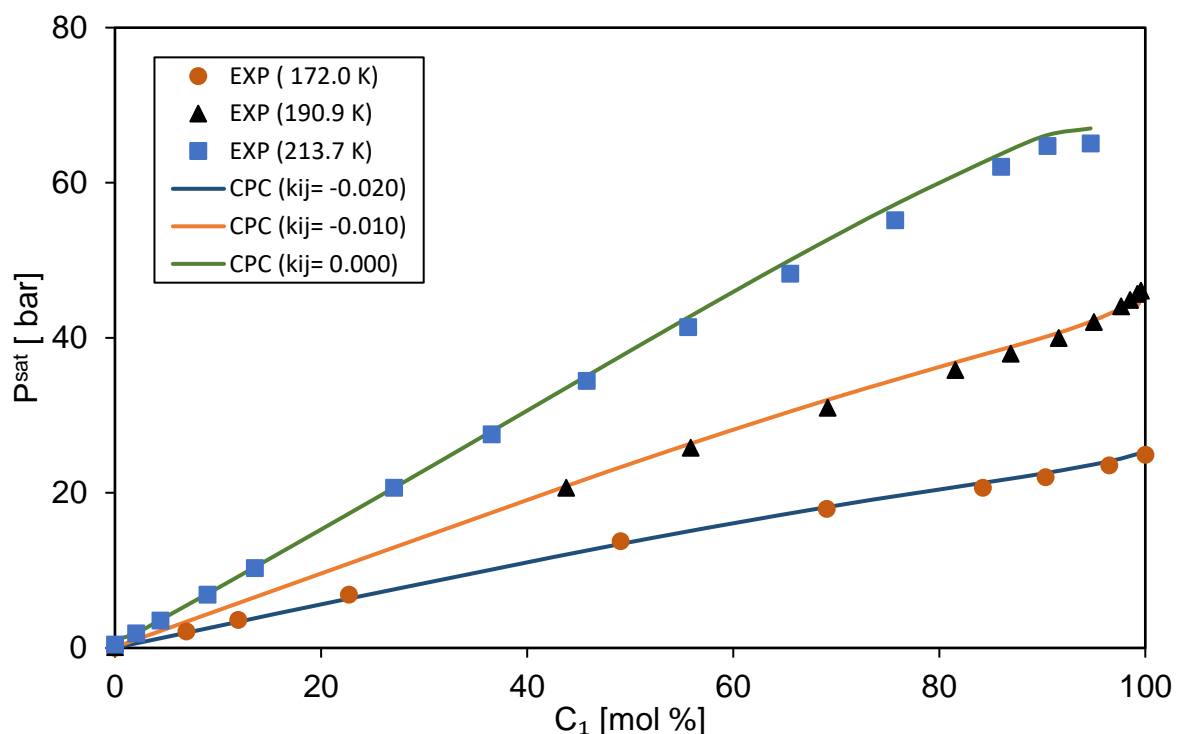

Figure 3.5.1. Vapor-Liquid Equilibrium (VLE) for Methane and Propane mixture with CPC at three different temperatures. Comparison of experimental data[64] to CPC calculations with different k_{ij} values.

Modeling vapor-liquid behavior of the second system that is illustrated in **Figure 3.5.1** shows how the CPC model can predict the phase behavior for three different temperature with three different binary interaction parameter values. The binary interaction parameter in this system increases with increasing the temperature. The reason that a negative k_{ij} used in this system is because of the overprediction of the bubble pressure (BP) by using the model in comparison with the experimental values obtained from the literature. When the k_{ij} is negative it leads to a higher molecular attraction term in

comparison with zero or positive k_{ij} values, and this leads to lower down the predicted saturation pressure since the second term in the CPC equation has a negative sign before it as explained in Chapter 2.

For the methane-propane mixture, the values of the binary interaction parameter show a linear trend with increasing the temperature. Therefore, a linear equation that connects these three data can be used to construct a linear equation that governs the relationship between the binary interaction parameter and the temperature as follows:

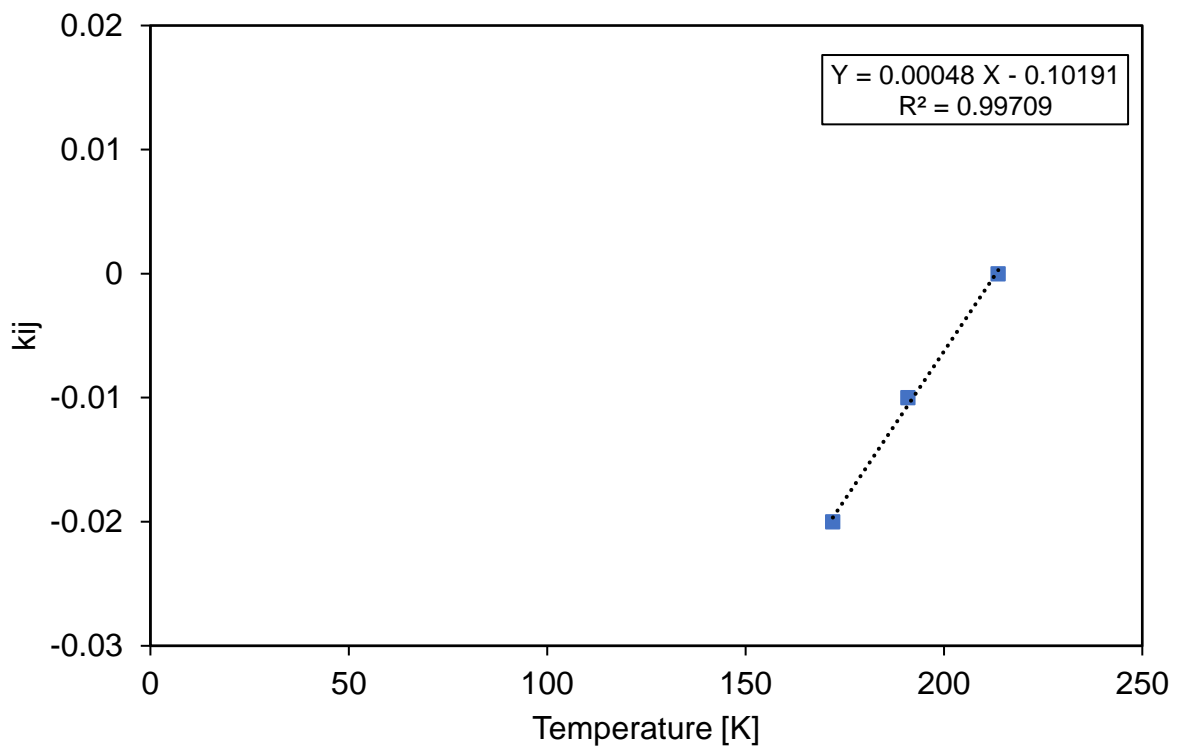**Figure 3.5.2.** A linear relation between the binary interaction parameter as a function of temperature for Methane-Propane mixture.

In **Figure 3.5.2,** the linear relation between k_{ij} and T was obtained by using three temperature values in a temperature range of 172.0 to 213.7 K. Since it shows a linear trend, the following equation will be general for a temperature inside that range or even

outside this range assuming the trend does not change. The Y in the linear equation represents the binary interaction parameter, and the X in the same equation represents the temperature in that system. The R^2 in the equation describes how closely the data comply with a linear relationship, and its value range from 0 to 1. A constant k_{ij} value was found and reported in **Table 3.3**, and it was found by reducing the average error between the experimental and the model saturation pressure values. Another example is a binary mixture consisting of hydrogen sulfide-propane mixture.
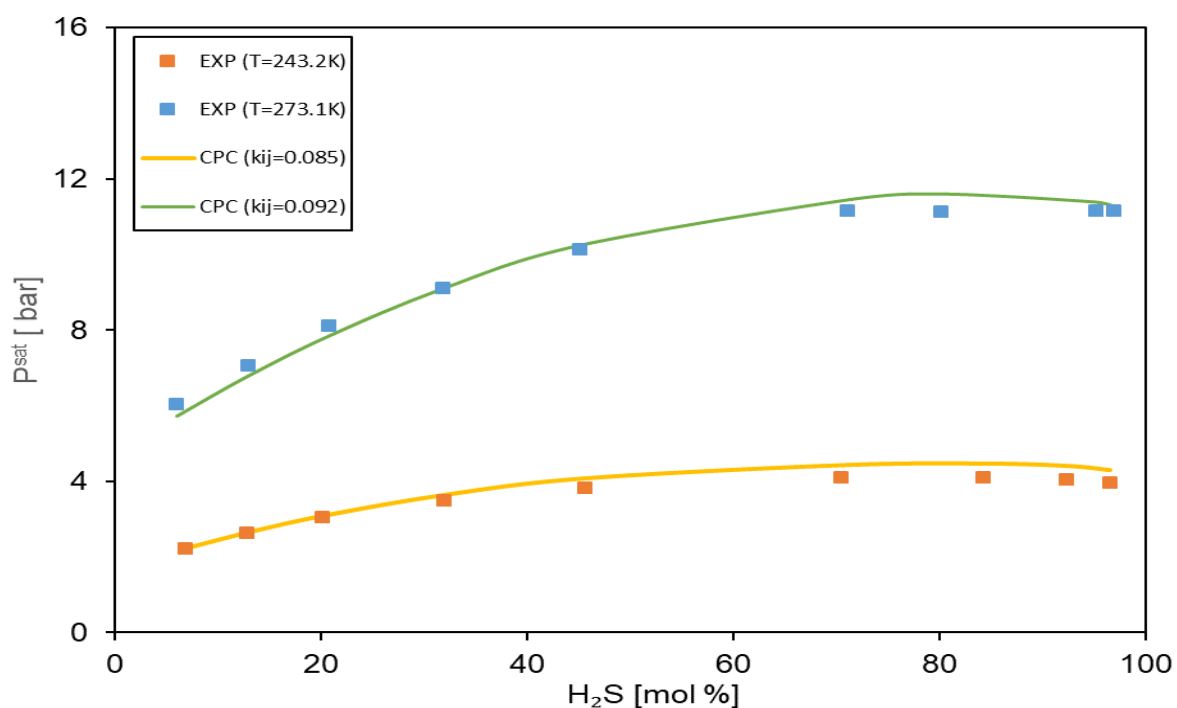
Figure 3.5.3. Vapor-Liquid Equilibrium (VLE) for Propane and Hydrogen Sulfide mixture with CPC at two different temperatures. Comparison of CPC calculations with different k_{ij} values with experimental data[65].

In **Figure 3.5.3**, the k_{ij} values increase with increasing temperatures in a temperature range of 223 K to 278 K. The graph shows how close the model to the experimental data by using three different k_{ij} values ranging from 0.060 to 0.080. The positive k_{ij} values

were required since the model underpredict the bubble pressure prediction because the molecular attraction term is lower than those with a k_{ij} of zero or negative values. This low molecular attraction parameter leads to having a higher bubble pressure. It worth noting that higher temperature leads to a higher deviation between the model and the experimental saturation pressure. Thus, an equation is proposed to describe the change in the k_{ij} as the temperature changes for this specific system, and it is shown in Appendix B. Similarly, hydrogen sulfide-methane and hydrogen sulfide-ethane mixtures were modeled with three different temperature values for each system. Again, three different values for the binary interaction parameter were observed as the temperature change. A constant k_{ij} value for those two systems are reported in **Table 3.3** for specific temperature ranges.

A mixture of carbon dioxide and hydrogen sulfide was modeled with two different temperature to obtain the bubble pressure for the mixture. The bubble pressure for the model underpredicts the experimental bubble pressure values that were obtained from the literature; thus, the binary interaction parameter was used to correct the prediction by adjusting the mixing rule for the molecular attraction parameter calculation. By using two k_{ij} values, the model prediction was enhanced to match the experimental data as shown in **Figure 3.5.4**.
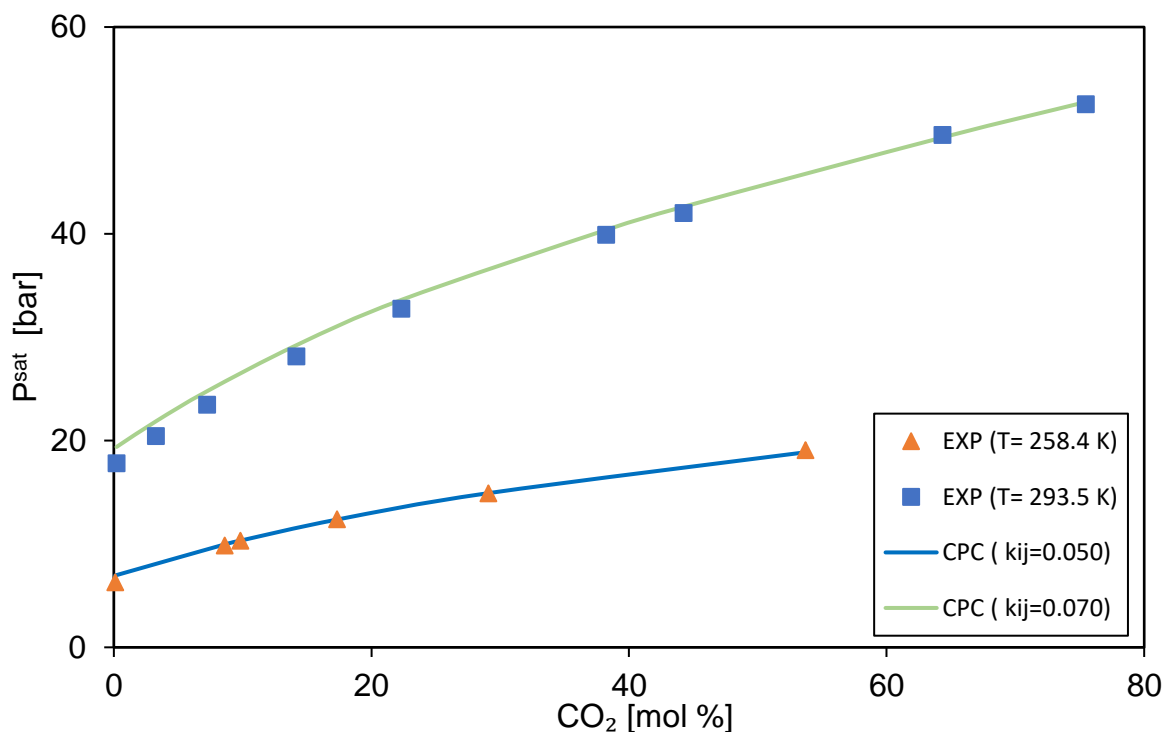
Figure 3.5.4. Vapor-Liquid Equilibrium (VLE) for a mixture of Carbon Dioxide and Hydrogen Sulfide with CPC at two different temperatures. Comparison of CPC calculations with different k_{ij} values to experimental data[66].

The prediction of the bubble pressure for $CO_2 - H_2S$ binary system is presented in figure above. The graphs show two different values for the binary interaction parameter with two different temperature values. In this case, as the temperature increases, it causes a model to have a higher deviation from the experimental values. Therefore, two different k_{ij} values were used to account for this deviation. Hence, as the temperature increases in a temperature range of 258.4 K to 293.5 K, the k_{ij} value increases at that range for this system. A constant value for a mixture of this system as well as carbon dioxide-methane, carbon dioxide-ethane, and carbon dioxide-propane systems are reported in **Table 3.3** for different ranges of temperature. A vapor-liquid equilibrium graph for carbon dioxide-

methane, and carbon dioxide-propane systems with different temperatures and k_{ij} values are shown in Appendix C.

A binary system consisting of nitrogen-carbon dioxide mixture was modeled with three different temperature ranging from 220-270 K. A negative binary interaction parameter was used for this system to lower down the prediction of the model since the model overpredicts the bubble pressure for this system. Again, the reason for this overprediction is because of the mixing rule failure in describing the interaction between the molecules of these two components.

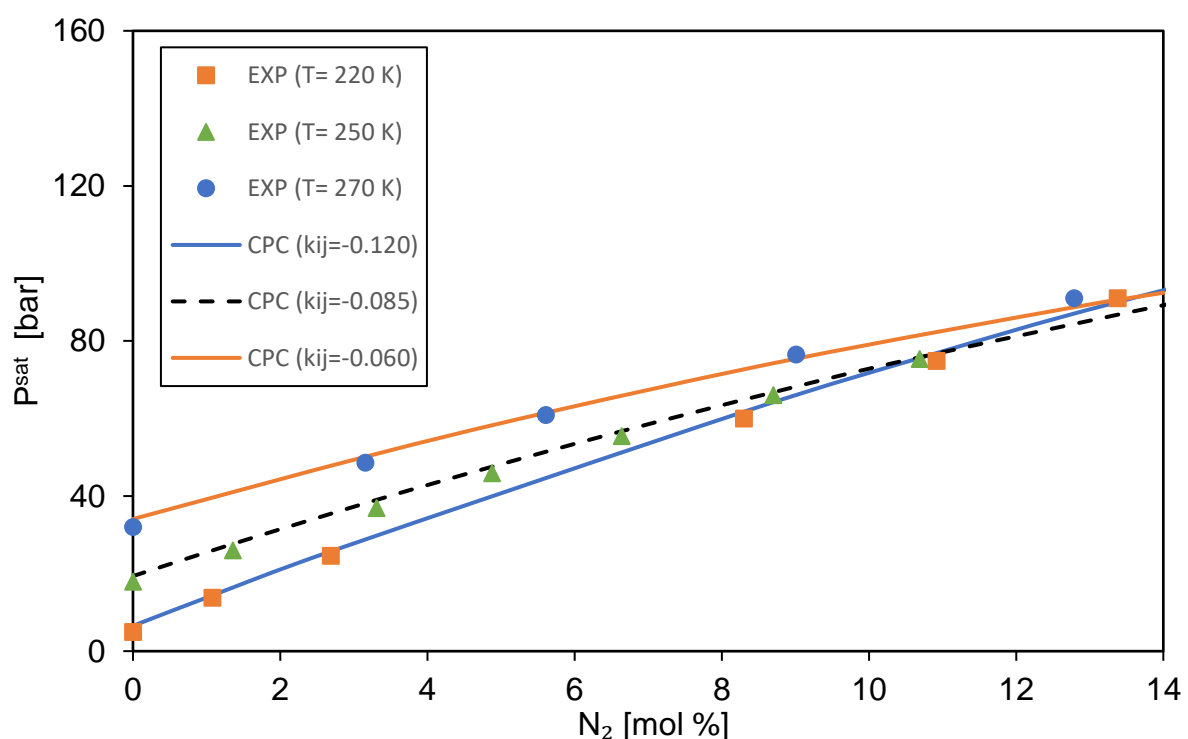**Figure 3.5.5.** Vapor-Liquid Equilibrium (VLE) for Carbon Dioxide and Nitrogen mixture with CPC at three different temperatures. Comparison of CPC calculations with different k_{ij} values to experimental data[67,68]

The vapor-liquid equilibrium behavior for the carbon dioxide and nitrogen binary system is depicted in **Figure 3.5.5**. The binary interaction parameter for this system increases

with increasing the temperature. A linear relationship can be obtained for this system at this temperature range by using the same approach as in **Figure 3.5.2** in order to account for the temperature inside this range or even extrapolate outside the range with a good prediction. A vapor-liquid equilibrium for nitrogen-methane, nitrogen-ethane, nitrogen-propane, and nitrogen-hydrogen sulfide are provided in Appendix C. In addition, a constant binary interaction parameter value for all of the 15 systems involved in this chapter are presented in **Table 3.3** for different temperature ranges. That was done by reducing the average error between the experimental lab data that were obtained from the literature, and the modeling prediction of the bubble pressure values.

Table 3.3. Constant Binary Interaction Values for Different Well-Defined Systems

Systems	Temperature Range (K)	k_{ij}
$N_2 - CH_4$	$122 - 128$	0.0110
$N_2 - C_2H_6$	$200 - 260$	0.0521
$N_2 - C_3H_8$	$260 - 270$	0.1400
$N_2 - H_2S$	$228 - 344$	0.1910
$N_2 - CO_2$	$220 - 270$	-0.1180
$CO_2 - CH_4$	$230 - 250$	0.0115
$CO_2 - C_2H_6$	$283 - 298$	0.0480
$CO_2 - C_3H_8$	$253 - 273$	0.0650
$CO_2 - H_2S$	$258 - 294$	0.0502
$H_2S - CH_4$	$223 - 278$	0.0656
$H_2S - C_2H_6$	$227 - 283$	0.0781
$H_2S - C_3H_8$	$243 - 283$	0.0907
$CH_4 - C_2H_6$	$172 - 200$	0.0000
$CH_4 - C_3H_8$	$172 - 214$	-0.0097
$C_2H_6 - C_3H_8$	$310 - 333$	0.0000

Table 3.3 presents the constant binary interaction parameter across different temperature ranges. If the model shows an optimal bubble pressure result when the binary interaction value is zero, it means that the model predicts the phase behavior efficiently without adding a correction to the mixing rule. However, when the k_{ij} value

deviates from zero, it means that the model does not describe the phase behavior correctly; hence a correction to the model is required. The highest k_{ij} value for those 15 systems in **Table 3.3** is for a mixture of nitrogen-hydrogen sulfide. On the other hand, the model shows to describe the phase behavior of methane-ethane and ethane-propane mixtures perfectly. Modeling the vapor-liquid equilibrium with the CPC equation for binary mixture involving nitrogen with another component that has a higher molecular weight seems to require a high k_{ij} value. For example, a constant value of k_{ij} for nitrogen-hydrogen sulfide mixture with using the CPC equation was found to be 0.191, which means the model does not describe the phase behavior correctly without adding this large correction. The same system was modeled with PC-SAFT under the same conditions, and it showed that PC-SAFT requires a high correction in modeling this system. The k_{ij} value for this system with using PC-SAFT equation was found to be 0.130. Similarly, modeling hydrogen sulfide-propane binary mixture shows to have a k_{ij} value of 0.0907 with using the CPC equation of state. The same system under the same conditions showed to have a binary interaction parameter value of 0.0712, which considered to be close to the value of the binary interaction parameter in the CPC equation. It worth noting that k_{ij} parameter in the CPC equation is a temperature dependent, and the reported constant k_{ij} values could get affected by changing the temperature ranges. Another reason for having such a high k_{ij} value could be because of the combining rules in the mixing rules that were used in the CPC equation. The combining rule for the interaction energy parameter is geometric-mean combining rule as shown in equation (2.67); whereas, the combining rule for the excluded volume parameter is a simple arithmetic-mean combining rule as described in equation (2.68).

When an arithmetic-mean combining rule is used in a quadratic mixing rule, it gives a linear mixing rule. Thus, this combining rule may not account for the cross volume correctly. It might be better to combine the diameter instead of volume because the combining rule in PC-SAFT accounts for combining diameters instead of volumes.

Chapter 4

Conclusions and Future Work

4.1. Conclusions

Modeling polymer systems with different solvents were proposed in this work. Different approaches in obtaining the pure component parameters for modeling polymers with the CPC equation were investigated. The phase behavior for polymer systems was modeled by using the CPC and the PC-SAFT equations of state. The PC-SAFT equation of state shows good results in modeling the cloud-point pressures by using a constant binary interaction parameter; however, the CPC equation required using temperature dependent binary interaction parameter to have similar results to PC-SAFT in modeling those systems. Those models were compared to experimental cloud points for different polymer-solvent systems available in the literature. Furthermore, the CPC equation showed to be faster than the PC-SAFT equation in terms of computational time. The combination of simplicity and speed is what makes the CPC equation of state to be attractive.

The effect of polydispersity, pressure, solvent types, temperature, polymer concentration, and molecular weight on phase behavior modeling were investigated. The CPC equation of state shows good correlations to the experimental data even though the solvent, temperature, polydispersity, and molecular weight are changed. Two different

systems were modeled to compare the cloud-point pressures for polymer assuming them to be monodisperse and polydisperse. The monodisperse polymer can have a good result for the given range of concentration if the binary interaction parameter is changed. A sensitivity analysis was performed to analyze which factor in the CPC equation has the highest impact on the modeling results, and Ω_B proved to have the highest effect on the cloud-point pressures. Moreover, the temperature dependency of the binary interaction parameter in the CPC equation of state was studied for polymer systems as well as 15 different well-defined systems. The results prove that the binary interaction parameter in the CPC equation of state is a temperature dependent parameter.

4.2. Recommendations and Future Work

Future work in the CPC equation of state is to test different radial distribution functions and different cubic equations of state forms other than Redlich-Kwong in modeling complex systems. Moreover, the excluded volume parameter (b_i) in the CPC equation lacks a temperature dependent term in comparison with the temperature dependent monomer segment diameter in the PC-SAFT equation. Therefore, the addition of a temperature dependent term and its effect on the temperature dependent binary interaction parameter needs to be investigated. In addition, different combining rules need to be analyzed in order to perfectly describe the cross volume of mixtures. The current combining rule in the CPC equation combines the volumes, whereas the combining rule in PC-SAFT is applied for diameters.

References

1. Yongcan Gao & Jiushun Zhang. Thermal cracking and catalytic cracking in fluid catalytic cracking process. *JOURNAL OF CHEMICAL INDUSTRY AND ENGINEERING* **53**, 469–472 (2002).

2. Walton, K. L., Clayfield, T., Hemphill, J. & Madenjian, L. Applications of Polyethylene Elastomers and Plastomers. in *Handbook of Industrial Polyethylene and Technology* 1197–1218 (John Wiley & Sons, Ltd, 2017). doi:10.1002/9781119159797.ch47

3. Baker, I. Polypropylene. in *Fifty Materials That Make the World* (ed. Baker, I.) 169–173 (Springer International Publishing, 2018). doi:10.1007/978-3-319-78766-4_32

4. Sisco, C. J., Abutaqiya, M. I. L., Vargas, F. M. & Chapman, W. G. Cubic-Plus-Chain (CPC). I: A SAFT-based Chain Modification to the Cubic Equation of State for Large Nonpolar Molecules. *Industrial & Engineering Chemistry Research* (2019). doi:10.1021/acs.iecr.9b00435

5. Chapman, W. G., Gubbins, K. E., Jackson, G. & Radosz, M. SAFT: Equation-of-state solution model for associating fluids. *Fluid Phase Equilibria* **52**, 31–38 (1989).

6. Chapman, W. G., Gubbins, K. E., Jackson, G. & Radosz, M. New reference equation of state for associating liquids. *Industrial & Engineering Chemistry Research* **29**, 1709–1721 (1990).

7. Legendre, A. M. *Traité des fonctions elliptiques et des intégrales Eulériennes: avec des tables pour en faciliter le calcul numérique. Contenant divers supplémens à la théorie des fonctions elliptiques*. (Huzard-Courcier, 1828).

8. Clapeyron, É. Mémoire sur la puissance motrice de la chaleur. *Journal de l'École polytechnique* **14**, 153–190 (1834).

9. Van Der Waals, J. D. The equation of state for gases and liquids. *Nobel Lecture* 254–265 (1910).

10. Redlich, O. & Kwong, J. N. S. On the Thermodynamics of Solutions. V. An Equation of State. Fugacities of Gaseous Solutions. *Chemical Reviews* **44**, 233–244 (1949).

11. Soave, G. Equilibrium constants from a modified Redlich-Kwong equation of state. *Chemical Engineering Science* (1971).

12. Peng, D.-Y. & Robinson, D. B. A New Two-Constant Equation of State. *Industrial & Engineering Chemistry Fundamentals* **15**, 59–64 (1976).

13. Wertheim, M. S. Fluids with highly directional attractive forces. I. Statistical thermodynamics. *J Stat Phys* **35**, 19–34 (1984).

14. Wertheim, M. S. Fluids with highly directional attractive forces. II. Thermodynamic perturbation theory and integral equations. *J Stat Phys* **35**, 35–47 (1984).

15. Wertheim, M. S. Fluids with highly directional attractive forces. III. Multiple attraction sites. *J Stat Phys* **42**, 459–476 (1986).

16. Wertheim, M. S. Fluids with highly directional attractive forces. IV. Equilibrium polymerization. *J Stat Phys* **42**, 477–492 (1986).

17. Economou, I. G. Statistical Associating Fluid Theory: A Successful Model for the Calculation of Thermodynamic and Phase Equilibrium Properties of Complex Fluid Mixtures. *Industrial & Engineering Chemistry Research* **41**, 953–962 (2002).

18. Huang, S. H. & Radosz, M. Equation of state for small, large, polydisperse, and associating molecules. *Industrial & Engineering Chemistry Research* **29**, 2284–2294 (1990).

19. Gross, J. & Sadowski, G. Application of perturbation theory to a hard-chain reference fluid: an equation of state for square-well chains. *Fluid Phase Equilibria* **168**, 183–199 (2000).

20. Gross, J. & Sadowski, G. Perturbed-Chain SAFT: An Equation of State Based on a Perturbation Theory for Chain Molecules. *Ind. Eng. Chem. Res.* **40**, 1244–1260 (2001).

21. Gross, J. & Sadowski, G. Modeling Polymer Systems Using the Perturbed-Chain Statistical Associating Fluid Theory Equation of State. *Ind. Eng. Chem. Res.* **41**, 1084–1093 (2002).

22. Gross, J. & Sadowski, G. Application of the Perturbed-Chain SAFT Equation of State to Associating Systems. *Ind. Eng. Chem. Res.* **41**, 5510–5515 (2002).

23. Barker, J. A. & Henderson, D. Perturbation Theory and Equation of State for Fluids: The Square-Well Potential. *J. Chem. Phys.* **47**, 2856–2861 (1967).

24. Barker, J. A. & Henderson, D. Perturbation Theory and Equation of State for Fluids. II. A Successful Theory of Liquids. *J. Chem. Phys.* **47**, 4714–4721 (1967).

25. Henderson, D. & Barker, J. A. Perturbation Theory and the Equation of State of Mixtures of Hard Spheres. *J. Chem. Phys.* **49**, 3377–3379 (1968).

26. Chen, S. S. & Kreglewski, A. Applications of the Augmented van der Waals Theory of Fluids.: I. Pure Fluids. *Berichte der Bunsengesellschaft für physikalische Chemie* **81**, 1048–1052 (1977).

27. Mansoori, G. A., Carnahan, N. F., Starling, K. E. & Leland, T. W. Equilibrium Thermodynamic Properties of the Mixture of Hard Spheres. *J. Chem. Phys.* **54**, 1523–1525 (1971).

28. Kontogeorgis, G. M., Voutsas, E. C., Yakoumis, I. V. & Tassios, D. P. An Equation of State for Associating Fluids. *Ind. Eng. Chem. Res.* **35**, 4310–4318 (1996).

29. Kontogeorgis, G. M. *et al.* Modelling of associating mixtures for applications in the oil & gas and chemical industries. *Fluid Phase Equilibria* **261**, 205–211 (2007).

30. Yan, W., Kontogeorgis, G. M. & Stenby, E. H. Application of the CPA equation of state to reservoir fluids in presence of water and polar chemicals. *Fluid Phase Equilibria* **276**, 75–85 (2009).

31. Li, Z. & Firoozabadi, A. Modeling Asphaltene Precipitation by n-Alkanes from Heavy Oils and Bitumens Using Cubic-Plus-Association Equation of State. *Energy Fuels* **24**, 1106–1113 (2010).

32. Tsivintzelis, I., Ali, S. & Kontogeorgis, G. M. Modeling Phase Equilibria for Acid Gas Mixtures using the Cubic-Plus-Association Equation of State. 3. Applications Relevant to Liquid or Supercritical CO2 Transport. *J. Chem. Eng. Data* **59**, 2955–2972 (2014).

33. Liang, X., Tsivintzelis, I. & Kontogeorgis, G. M. Modeling Water Containing Systems with the Simplified PC-SAFT and CPA Equations of State. *Ind. Eng. Chem. Res.* **53**, 14493–14507 (2014).

34. Arya, A., von Solms, N. & Kontogeorgis, G. M. Determination of asphaltene onset conditions using the cubic plus association equation of state. *Fluid Phase Equilibria* **400**, 8–19 (2015).

35. Arya, A., von Solms, N. & Kontogeorgis, G. M. Investigation of the Gas Injection Effect on Asphaltene Onset Precipitation Using the Cubic-Plus-Association Equation of State. *Energy Fuels* **30**, 3560–3574 (2016).

36. Elliott, J. R., Suresh, S. J. & Donohue, M. D. A simple equation of state for non-spherical and associating molecules. *Industrial & Engineering Chemistry Research* **29**, 1476–1485 (1990).

37. Sako, T., Wu, A. H. & Prausnitz, J. M. A cubic equation of state for high-pressure phase equilibria of mixtures containing polymers and volatile fluids. *Journal of Applied Polymer Science* **38**, 1839–1858 (1989).

38. Kontogeorgis, G. M., Harismiadis, V. I., Fredenslund, A. & Tassios, D. P. Application of the van der Waals equation of state to polymers: I. Correlation. *Fluid Phase Equilibria* **96**, 65–92 (1994).

39. Harismiadis, V. I., Kontogeorgis, G. M., Fredenslund, A. & Tassios, D. P. Application of the van der Waals equation of state to polymers: II. Prediction. *Fluid Phase Equilibria* **96**, 93–117 (1994).

40. Harismiadis, V. I., Kontogeorgis, G. M., Saraiva, A., Fredenslund, A. & Tassios, D. P. Application of the van der Waals equation of state to polymers III. Correlation and prediction of upper critical solution temperatures for polymer solutions. *Fluid Phase Equilibria* **100**, 63–102 (1994).

41. Saraiva, A., Kontogeorgis, G. M., Harismiadis, V. J., Fredenslund, A. & Tassios, D. P. Application of the van der Waals equation of state to polymers IV. Correlation and prediction of lower critical solution temperatures for polymer solutions. *Fluid Phase Equilibria* **115**, 73–93 (1996).

42. Harismiadis, V. I. *et al.* Miscibility of polymer blends with engineering models. *AIChE Journal* **42**, 3170–3180 (1996).

43. Bithas, S. G., Kalospiros, N. S., Kontogeorgis, G. M. & Tassios, D. Henry constants in polymer solutions with the van der waals equation of state. *Polymer Engineering & Science* **36**, 254–261 (1996).

44. Louli, V. & Tassios, D. Vapor–liquid equilibrium in polymer–solvent systems with a cubic equation of state. *Fluid Phase Equilibria* **168**, 165–182 (2000).

45. Stryjek, R. & Vera, J. H. PRSV: An improved peng—Robinson equation of state for pure compounds and mixtures. *The Canadian Journal of Chemical Engineering* **64**, 323–333 (1986).

46. Orbey, N. & Sandler, S. I. Vapor-liquid equilibrium of polymer solutions using a cubic equation of state. *AIChE Journal* **40**, 1203–1209 (1994).

47. Wong, D. S. H. & Sandler, S. I. A theoretically correct mixing rule for cubic equations of state. *AIChE Journal* **38**, 671–680 (1992).

48. Zhong, C. & Masuoka, H. A new mixing rule for cubic equations of state and its application to vapor-liquid equilibria of polymer solutions. *Fluid Phase Equilibria* **123**, 59–69 (1996).

49. Gupta, R. B. & Prausnitz, J. M. Vapor–Liquid Equilibria for Solvent–Polymer Systems from a Perturbed Hard-Sphere-Chain Equation of State. *Ind. Eng. Chem. Res.* **35**, 1225–1230 (1996).

50. Costa, G. M. N. *et al.* Modeling of solid–liquid equilibria for polyethylene and polypropylene solutions with equations of state. *Journal of Applied Polymer Science* **121**, 1832–1849 (2011).

51. Clayman, H. M. Polypropylene. *Ophthalmology* **88**, 959–964 (1981).

52. Martin, T. M., Lateef, A. A. & Roberts, C. B. Measurements and modeling of cloud point behavior for polypropylene/n-pentane and polypropylene/n-pentane/carbon dioxide mixtures at high pressure. *Fluid Phase Equilibria* **154**, 241–259 (1999).

53. Whaley, P. D., Winter, H. H. & Ehrlich, P. Phase Equilibria of Polypropylene with Compressed Propane and Related Systems. 1. Isotactic and Atactic Polypropylene with Propane and Propylene. *Macromolecules* **30**, 4882–4886 (1997).

54. Osman, M. A., Rupp, J. E. P. & Suter, U. W. Tensile properties of polyethylene-layered silicate nanocomposites. *Polymer* **46**, 1653–1660 (2005).

55. Pechmann, H. v. Ueber Diazomethan und Nitrosoacylamine. *Berichte der deutschen chemischen Gesellschaft* **31**, 2640–2646 (1898).

56. De Loos, T. W., Poot, W. & Diepen, G. A. M. Fluid phase equilibriums in the system polyethylene + ethylene. 1. Systems of linear polyethylene + ethylene at high pressure. *Macromolecules* **16**, 111–117 (1983).

57. HAO, W. Polymer Solution Data Collection, Part I Vapor-Liquid Equilibrium. *DECHEMA Chemistry Data Series* (1992).

58. Kiran, E., Xiong, Y. & Zhuang, W. Effect of polydispersity on the demixing pressures of polyethylene in near- or supercritical alkanes. *The Journal of Supercritical Fluids* **7**, 283–287 (1994).

59. Wohlfarth, C. *Vapour-Liquid Equilibrium Data of Binary Polymer Solutions: Vapour Pressures, Henry-Constants and Segment-Molar Excess Gibbs Free Energies*. (Elsevier Science, 1994).

60. Mueller, C. Untersuchungen zum Phasenverhalten von quasibinaren Gemischen aus Ethylen und Ethylen-Copolymeren. (Karlsruhe, 1996).

61. Simon, E. Ueber den flüssigen Storax (Styrax liquidus). *Ann. Pharm* **31**, 265–277 (1839).

62. McKeen, L. W. 3 - Plastics Used in Medical Devices. in *Handbook of Polymer Applications in Medicine and Medical Devices* (eds. Modjarrad, K. & Ebnesajjad, S.) 21–53 (William Andrew Publishing, 2014). doi:10.1016/B978-0-323-22805-3.00003-7

63. Sadowski, G., Mokrushina, L. V. & Arlt, W. Finite and infinite dilution activity coefficients in polycarbonate systems. *Fluid Phase Equilibria* **139**, 391–403 (1997).

64. Wichterle, I. & Kobayashi, R. Vapor-liquid equilibrium of methane-propane system at low temperatures and high pressures. *Journal of Chemical & Engineering Data* **17**, 4–9 (1972).

65. Steckel, F. Vapor-liquid equilibria under pressure of some binary hydrogen sulfide-containing systems. *Sven Kem Tidskr* **57**, 209–216 (1945).

66. Chapoy, A., Coquelet, C., Liu, H., Valtz, A. & Tohidi, B. Vapour–liquid equilibrium data for the hydrogen sulphide (H2S)+carbon dioxide (CO2) system at temperatures from 258 to 313K. *Fluid Phase Equilibria* **356**, 223–228 (2013).

67. Brown, T. S., Sloan, E. D. & Kidnay, A. J. Vapor-liquid equilibria in the nitrogen + carbon dioxide + ethane system. *Fluid Phase Equilibria* **51**, 299–313 (1989).

68. Brown, T. S., Niesen, V. G., Sloan, E. D. & Kidnay, A. J. Vapor-liquid equilibria for the binary systems of nitrogen, carbon dioxide, and n-butane at temperatures from 220 to 344 K. *Fluid Phase Equilibria* **53**, 7–14 (1989).

69. Wichterle, I. & Kobayashi, R. Vapor-liquid equilibrium of methane-ethane system at low temperatures and high pressures. *Journal of Chemical & Engineering Data* **17**, 9–12 (1972).

70. Matschke, D. E. & Thodos, G. Vapor-Liquid Equilibria for the Ethane-Propane System. *Journal of Chemical & Engineering Data* **7**, 232–234 (1962).

71. Privat, R., Mutelet, F. & Jaubert, J.-N. Addition of the Hydrogen Sulfide Group to the PPR78 Model (Predictive 1978, Peng–Robinson Equation of State with Temperature Dependent kij Calculated through a Group Contribution Method). *Ind. Eng. Chem. Res.* **47**, 10041–10052 (2008).

72. Bian, B., Wang, Y., Shi, J., Zhao, E. & Lu, B. C.-Y. Simultaneous determination of vapor-liquid equilibrium and molar volumes for coexisting phases up to the critical temperature with a static method. *Fluid Phase Equilibria* **90**, 177–187 (1993).

73. Kim, J. H. & Kim, M. S. Vapor–liquid equilibria for the carbon dioxide+propane system over a temperature range from 253.15 to 323.15K. *Fluid Phase Equilibria* **238**, 13–19 (2005).

74. Stryjek, R., Chappelear, P. S. & Kobayashi, R. Low-temperature vapor-liquid equilibriums of nitrogen-methane system. *Journal of Chemical & Engineering Data* **19**, 334–339 (1974).

75. Das, T. R. & Eubank, P. T. Thermodynamic Properties of Propane: Vapor-Liquid Coexistence Curve. in *Advances in Cryogenic Engineering* (ed. Timmerhaus, K. D.) 208–219 (Springer US, 1973).

76. Potoff, J. J. & Siepmann, J. I. Vapor–liquid equilibria of mixtures containing alkanes, carbon dioxide, and nitrogen. *AIChE Journal* **47**, 1676–1682 (2001).

77. Besserer, G. J. & Robinson, D. B. Equilibrium-phase properties of nitrogen-hydrogen sulfide system. *Journal of Chemical & Engineering Data* **20**, 157–161 (1975).

Appendix A

Relating the change in entropy equation to equilibrium conditions. The necessary equations in calculating the Ω_A and Ω_B in the CPC equation of state.

Derivation of equilibrium conditions by entropy maximization approach:

$$dU = TdS - PdV + \sum_{i=1}^{N_C} \mu_i \, dn_i \qquad (A.1)$$

By rearranging the equation above:

$$dS = \frac{1}{T}dU + \frac{P}{T}dV - \frac{1}{T}\sum_{i=1}^{N_C} \mu_i dn_i \qquad (A.2)$$

For an isolated system where neither energy and matter can enter or escape the system:

$$dV = dV^\alpha + dV^\beta = 0 \qquad (A.3)$$

$$dn = dn^\alpha + dn^\beta = 0 \qquad (A.4)$$

$$dU = 0 \qquad (A.5)$$

Then equation (A.2) can be rewritten as:

$$dS = \frac{P^\alpha}{T^\alpha}dV^\alpha - \frac{1}{T^\alpha}\sum_{i=1}^{N_C} \mu_i^\alpha dn_i^\alpha - \frac{P^\beta}{T^\beta}dV^\alpha + \frac{1}{T^\beta}\sum_{i=1}^{N_C} \mu_i^\beta dn_i^\alpha = 0 \qquad (A.6)$$

Temperature, pressure, and chemical potential in both phases needs to be equal in order to satisfy the equation above.

The expressions for calculating β_c and Z_c in equations (2.69) and (2.70) for CPC[4] are given by:

$$Z_c = m Z_c^{mono} - (m-1) Z_c^{chain} \tag{A.7}$$

Where Z_c^{mono} and Z_c^{chain} are calculated by the following experessions:

$$Z_c^{mono} = \frac{1}{1-\beta_c}\left[1 + \frac{\beta_c}{\lambda^{mono}(1+\beta_c)}\right]^{-1} \tag{A.8}$$

$$Z_c^{chain} = \frac{\beta_c}{1+\beta_c}\left[\frac{\lambda^{chain}}{\lambda^{mono}} + \frac{40}{(40-19\,\beta_c)}\left[1 + \frac{\beta_c}{\lambda^{mono}(1+\beta_c)}\right]^{-1}\right] \tag{A.9}$$

Both of λ^{mono} and λ^{chain} are expressed as follows:

$$\lambda^{mono} = -\beta_c \frac{\beta_c^2 + 2\beta_c - 1}{(1+\beta_c)^2} \tag{A.10}$$

$$\lambda^{chain} = \frac{840\beta_c}{(40-19\beta_c)^2} \tag{A.11}$$

$$\Omega_a(m) = \frac{1}{m^2}\left[\frac{\beta_c Z_c^2}{\lambda^{mon}} + (m-1)\beta_c Z_c \frac{\lambda^{chain}}{\lambda^{mon}}\right] \tag{A.12}$$

$$\Omega_b(m) = \frac{1}{m}\beta_c Z_c \tag{A.13}$$

Table A.1. Coefficients for 6th order polynomial for solving β_c for CPC[4].

Coefficient	Expression
c_0	$-128{,}000 - 128{,}000\,m_0$
c_1	$566{,}400 + 566{,}400\,m_0$
c_2	$-249{,}840 - 748{,}800\,m_0$
c_3	$-145{,}562 + 188{,}800\,m_0$
c_4	$36{,}366 + 182{,}400\,m_0$
c_5	$45{,}486$
c_6	$-13{,}718 - 60{,}800\,m_0$

Appendix B

Pure-component parameters for polymers that were used in PC-SAFT modeling as well as CPC modeling, the polydispersity for polypropylene and LDPE polymers, pure-component parameters for different solvents, and linear relation between k_{ij} and T for different binary mixtures

Table B.1. Pure-Component Parameters for Polymers Modeling with PC-SAFT[21]

Systems	m/M_w $[mol/g]$	σ_j [Å]	ϵ_j/k [K]
Polypropylene	0.02305	4.1	217.0
HDPE	0.0263	4.0217	252.0
LDPE	0.0263	4.0217	249.5
Polystyrene	0.0190	4.1071	267.0

Table B.2. Pure-Component Parameters for the Reference Monomers in Modeling with CPC

Reference Monomer	M_W $[g/mol]$	T_c $[K]$	P_c $[bar]$	m_{mono} $[-]$
Ethane	30.070	305.3	48.72	1.3301
Propane	44.096	369.8	42.48	1.7047
Styrene	104.15	636.00	38.40	3.3500

Table B.3. Molecular Weight Distribution of Three Pseudo-Components of PP[53]

Pseudo-Component	Mol wt M_j $[\frac{g}{mol}]$	Weight fraction w_{pj}
1	35760.835	0.508437583
2	504683.77	0.479290585
3	2438722.87	0.012271832

Table B.4. Molecular Weight Distribution of six Pseudo-Components of LDPE[60]

Pseudo-component	Mol wt M_j $[\frac{g}{mol}]$	Weight fraction w_{pj}
1	2570	0.1136765
2	76200	0.4774815
3	244000	0.317655
4	513000	0.0821108
5	899000	0.0087705
6	1450000	0.0003057

Table B.5. Pure-Component Parameters for Different Solvents in Modeling with CPC[4]

Solvents	M_W (g/mol)	T_c (K)	P_c (bar)	m
Ethylene	28.053	282.4	50.6	1.028
Propane	44.096	369.8	42.48	1.7047
n-Pentane	72.146	469.7	33.70	2.6278
Toluene	92.141	591.75	41.08	3.0329
Ethylbenzene	106.165	617.2	36.06	3.4995

Table B.6. Relation Between Binary Interaction Parameter and Temperature of CPC for Polymer-Solvent Mixtures

Systems	Temperature Range (°C)	Linear Equation Relating $(k_{ij} - T)$
Polypropylene-Propane	$135 - 155$	$k_{ij} = 0.0003\,T + 0.0130$
Polypropylene-n-Pentane	$177 - 197$	$k_{ij} = 0.0011\,T - 0.1767$
HDPE-Ethylene	$140 - 170$	$k_{ij} = 0.0002\,T - 0.0031$
LDPE-Ethylene	$150 - 250$	$k_{ij} = 0.0001\,T + 0.0030$

Table B.7. Relation Between Binary Interaction Parameter and Temperature of CPC for Different Selected Binary Mixtures

Systems	Temperature Range (K)	Linear Equation Relating $(k_{ij} - T)$
$N_2 - C_2H_6$	$200 - 260$	$k_{ij} = 0.0013\,T - 0.2233$
$N_2 - H_2S$	$228 - 344$	$k_{ij} = 0.0008\,T + 0.0022$
$N_2 - CO_2$	$220 - 270$	$k_{ij} = 0.0012\,T - 0.3859$
$H_2S - CH_4$	$223 - 278$	$k_{ij} = 0.0004\,T - 0.0171$
$H_2S - C_2H_6$	$227 - 283$	$k_{ij} = -0.0002\,T + 0.1213$
$CH_4 - C_3H_8$	$172 - 214$	$k_{ij} = 0.0005\,T - 0.1019$

Appendix C

Vapor-liquid equilibrium for different systems by using CPC equation of state. The following results show that CPC requires using temperature dependent binary interaction parameter.
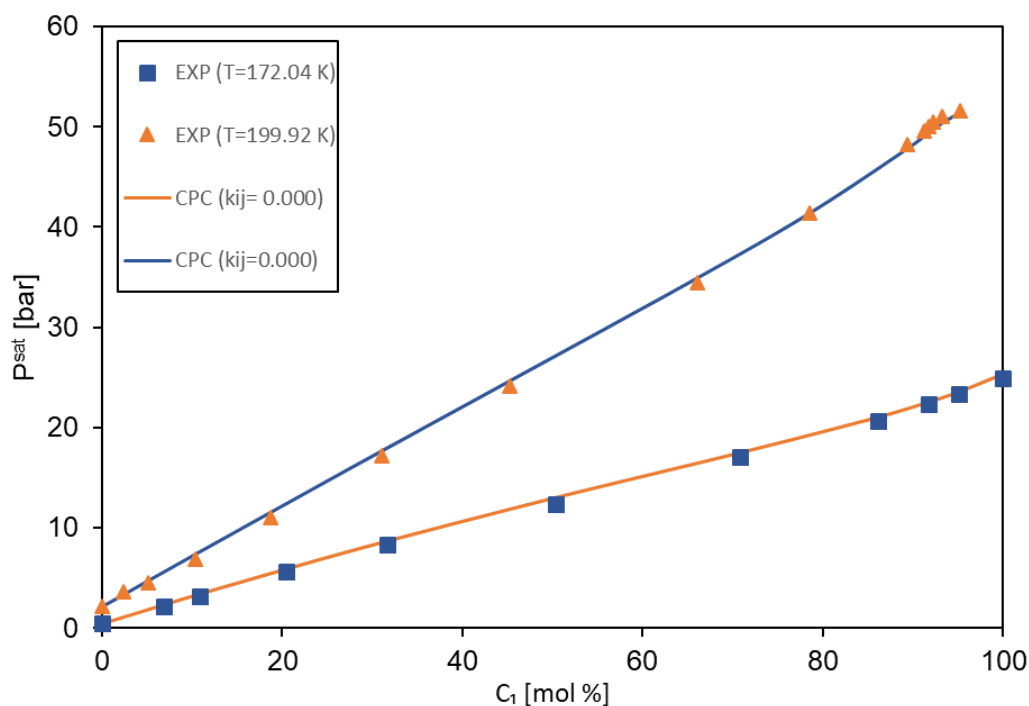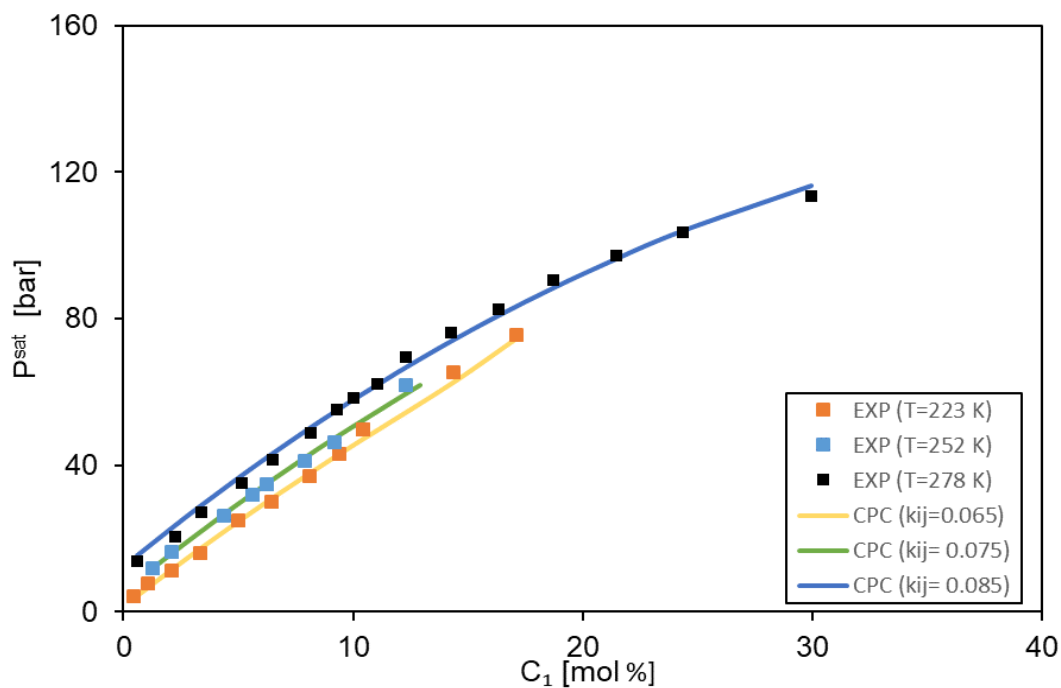

Figure C.1. Vapor-Liquid Equilibrium (VLE) for Methane and Ethane mixture with CPC at two different temperatures. Comparison of experimental data[69] to CPC calculations with ($k_{ij} = 0.000$).
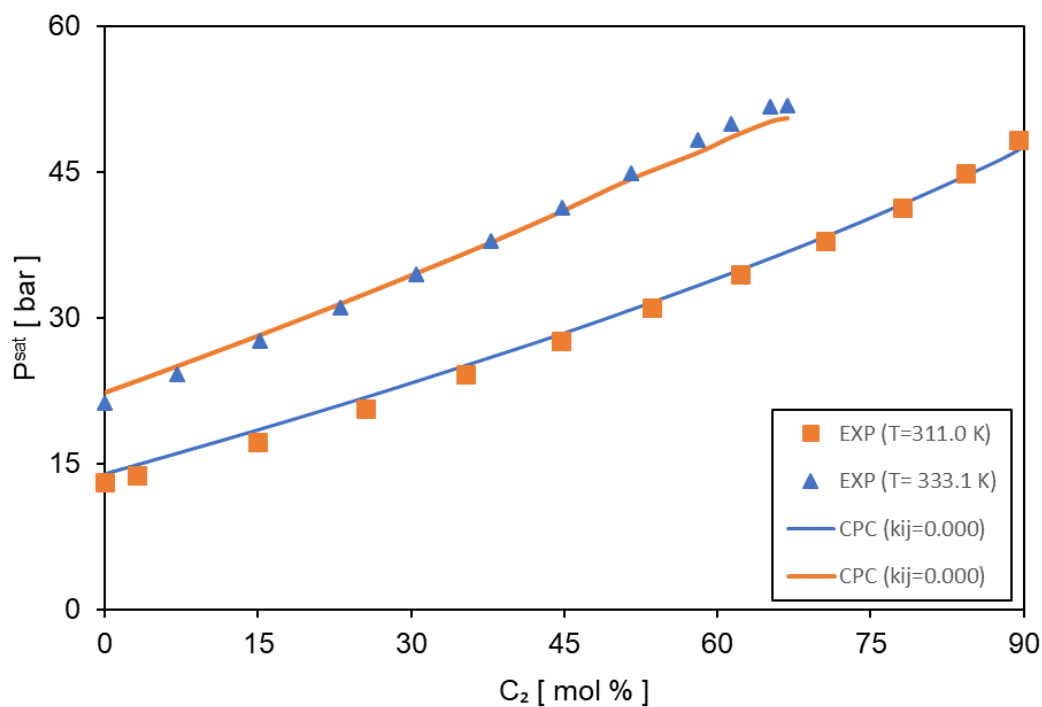
Figure C.2. Vapor-Liquid Equilibrium (VLE) for Ethane and Propane mixture with CPC at two different temperatures. Comparison of CPC calculations with different k_{ij} values with experimental data[70].
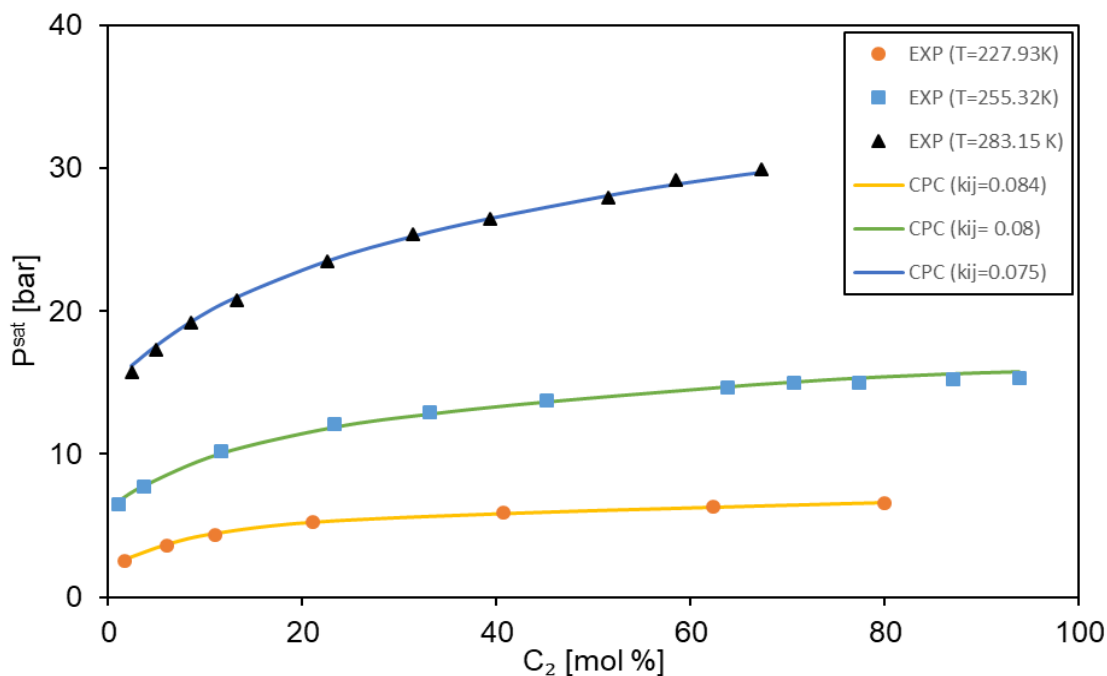

Figure C.3. Vapor-Liquid Equilibrium (VLE) for Hydrogen Sulfide and Methane mixture with CPC at three different temperatures. Comparison of CPC calculations with different k_{ij} values to experimental data[71].
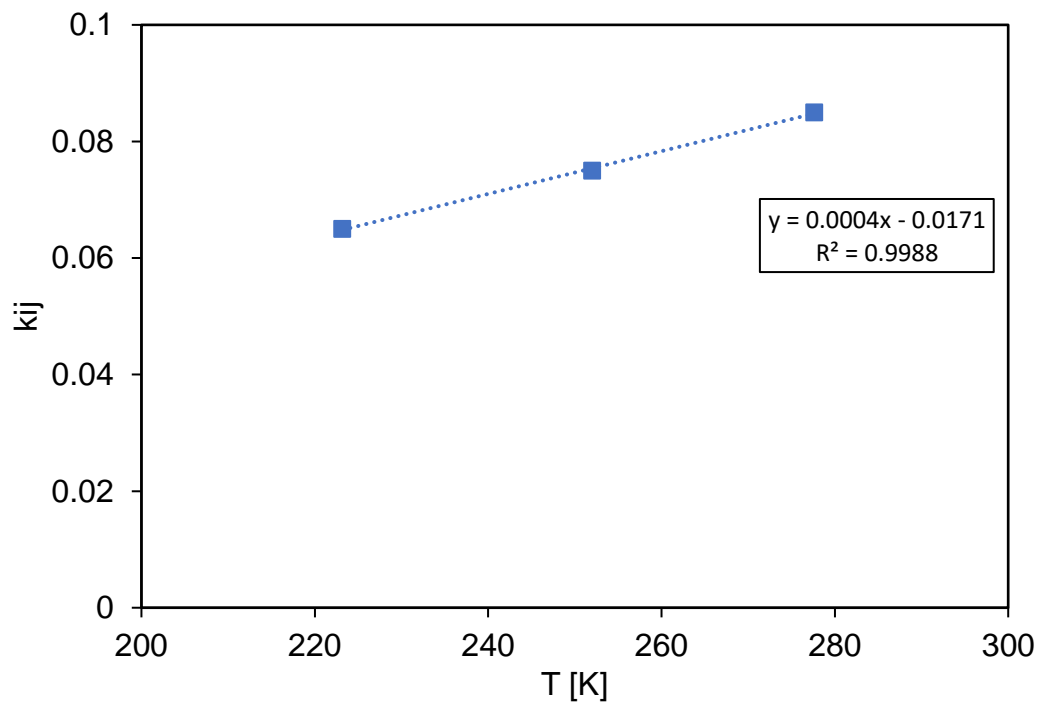
Figure C.4. A linear relation between the binary interaction parameter as a function of temperature for Hydrogen Sulfide-Methane mixture.
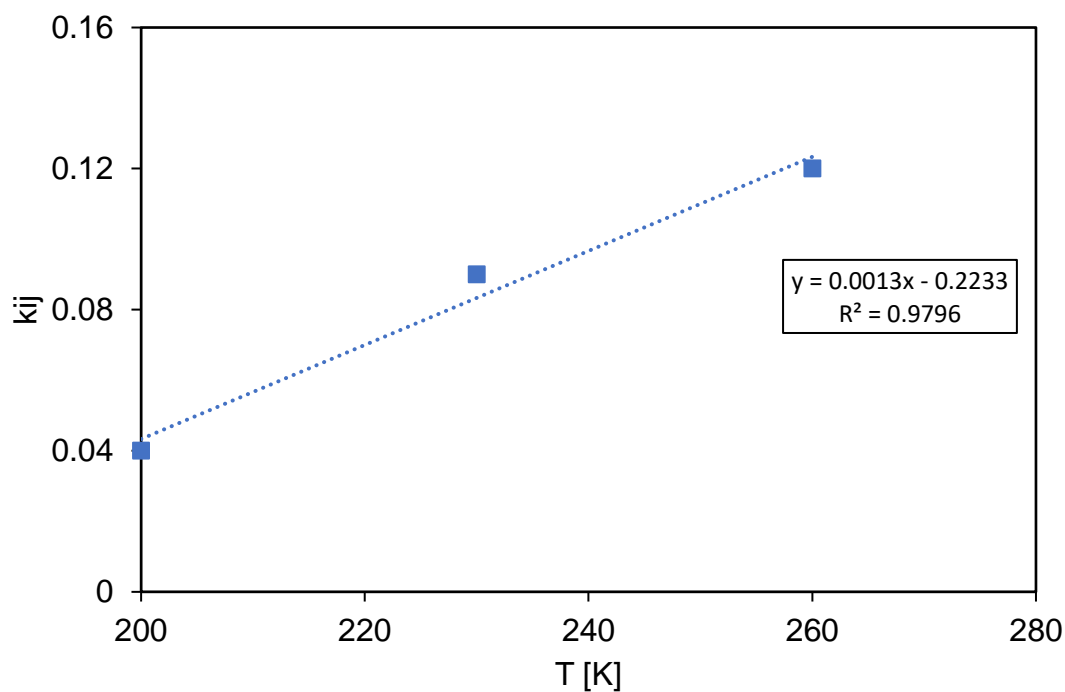
Figure C.5. A linear relation between the binary interaction parameter as a function of temperature for Nitrogen-Ethane mixture.

Figure C.6. Vapor-Liquid Equilibrium (VLE) for Hydrogen Sulfide and Ethane mixture with CPC at three different temperatures. Comparison of CPC calculations with different k_{ij} values to experimental data[71].
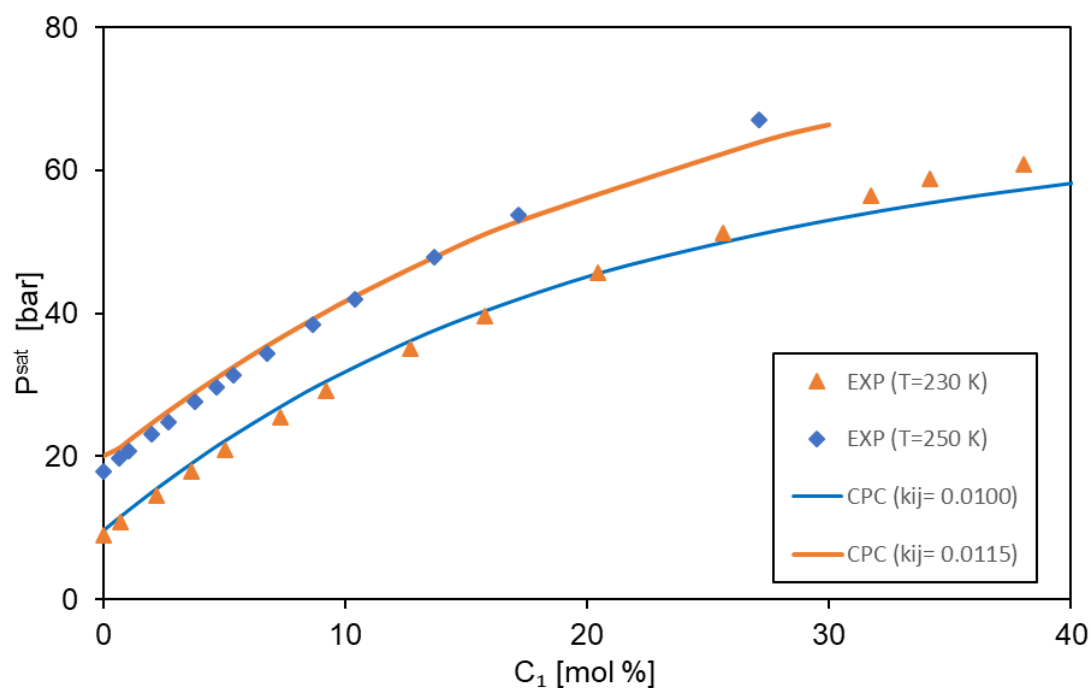
Figure C.7. Vapor-Liquid Equilibrium (VLE) for Methane and Carbon Dioxide mixture with CPC at two different temperatures. Comparison of CPC calculations with different k_{ij} values with experimental data[72].
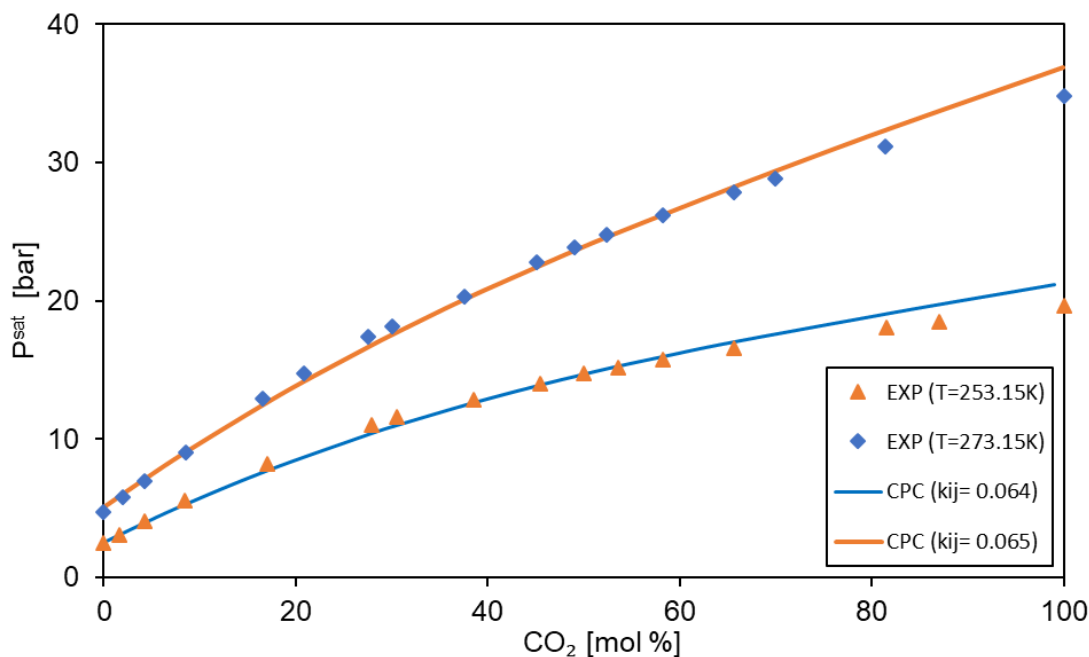
Figure C.8. Vapor-Liquid Equilibrium (VLE) for Propane and Carbon Dioxide mixture with CPC at two different temperatures. Comparison of CPC calculations with different k_{ij} values with experimental data[73].
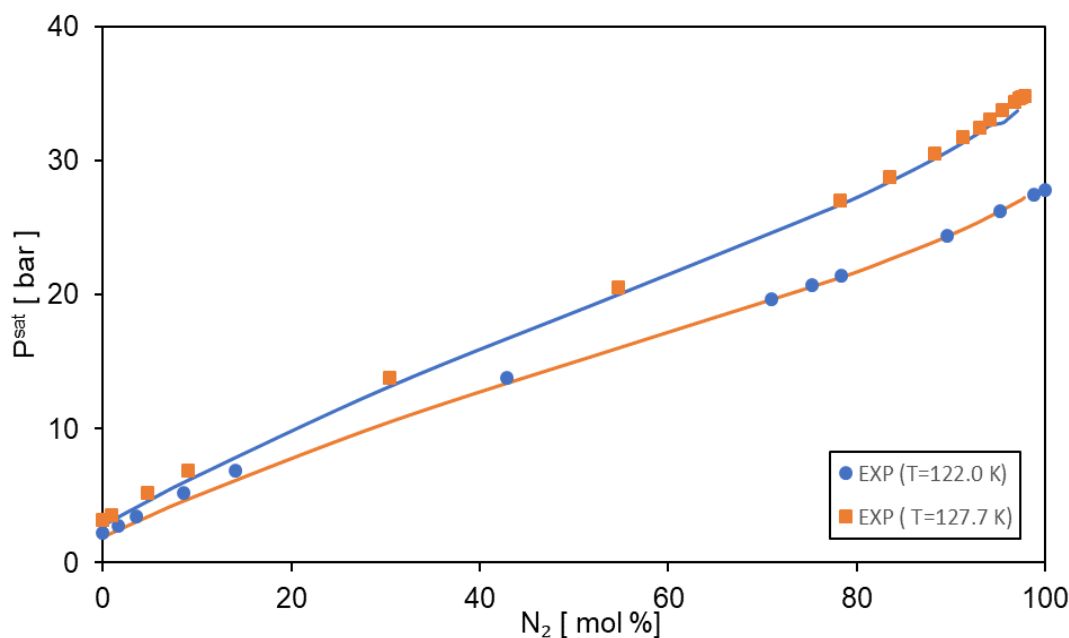

Figure C.9. Vapor-Liquid Equilibrium (VLE) for Nitrogen and Methane mixture with CPC at two different temperatures. Comparison of CPC calculations with experimental data[74].
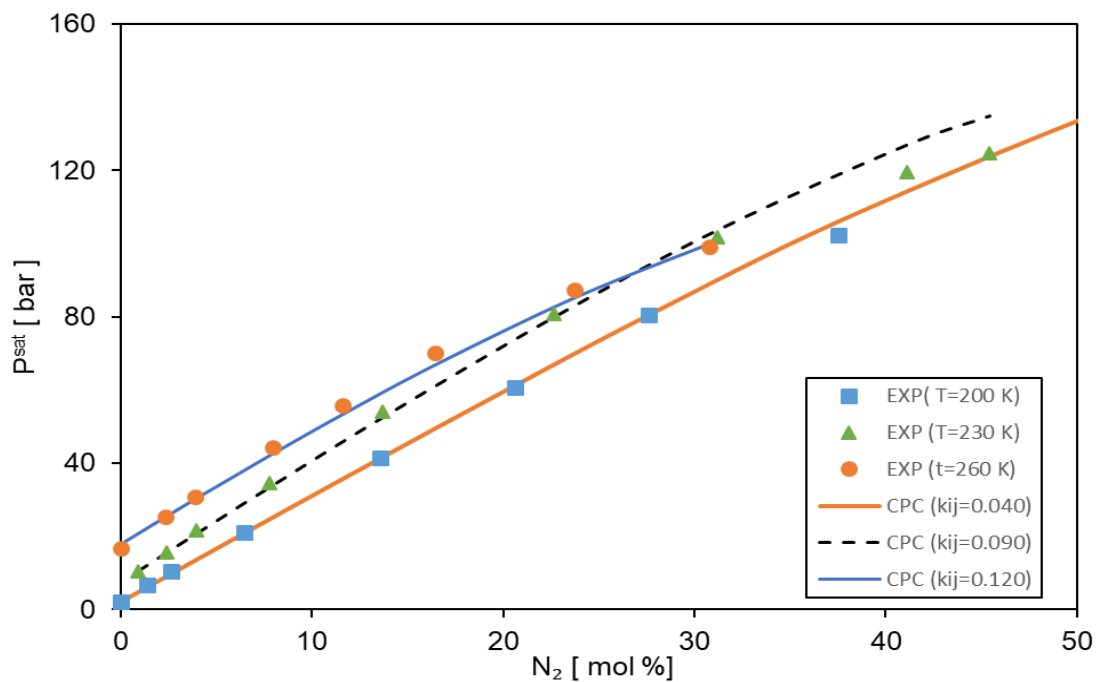
Figure C.10. Vapor-Liquid Equilibrium (VLE) for Nitrogen and Ethane mixture with CPC at three different temperatures. Comparison of CPC calculations with different k_{ij} values with experimental data[75].
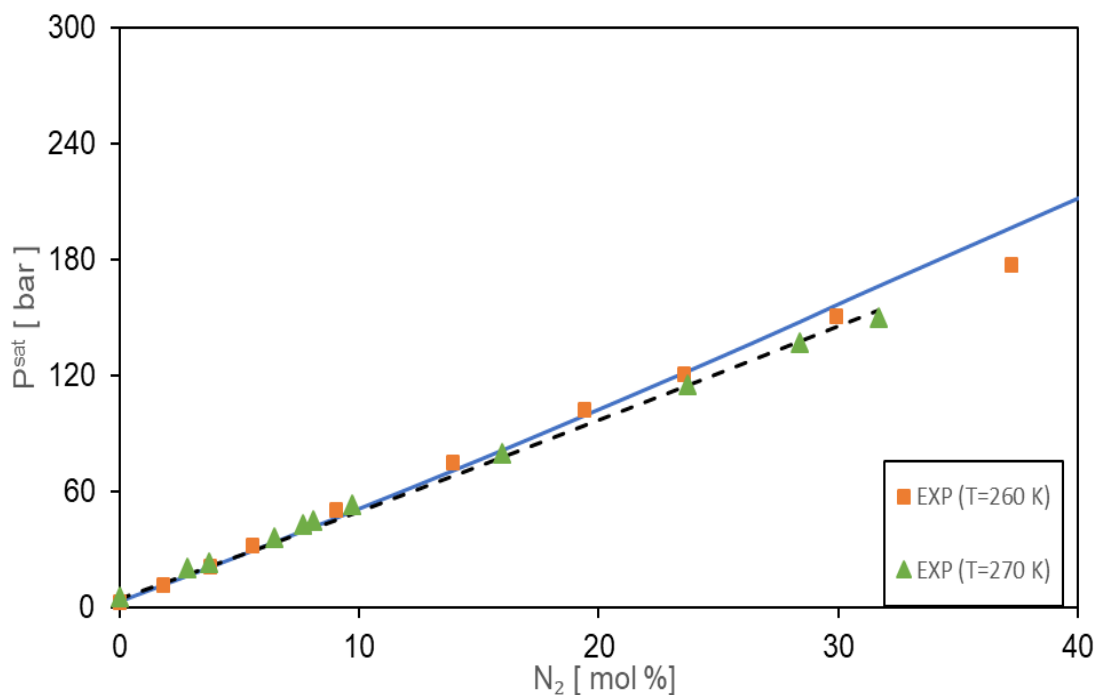

Figure C.11. Vapor-Liquid Equilibrium (VLE) for Nitrogen and Propane mixture with CPC at two different temperatures. Comparison of CPC calculations with experimental data[76].
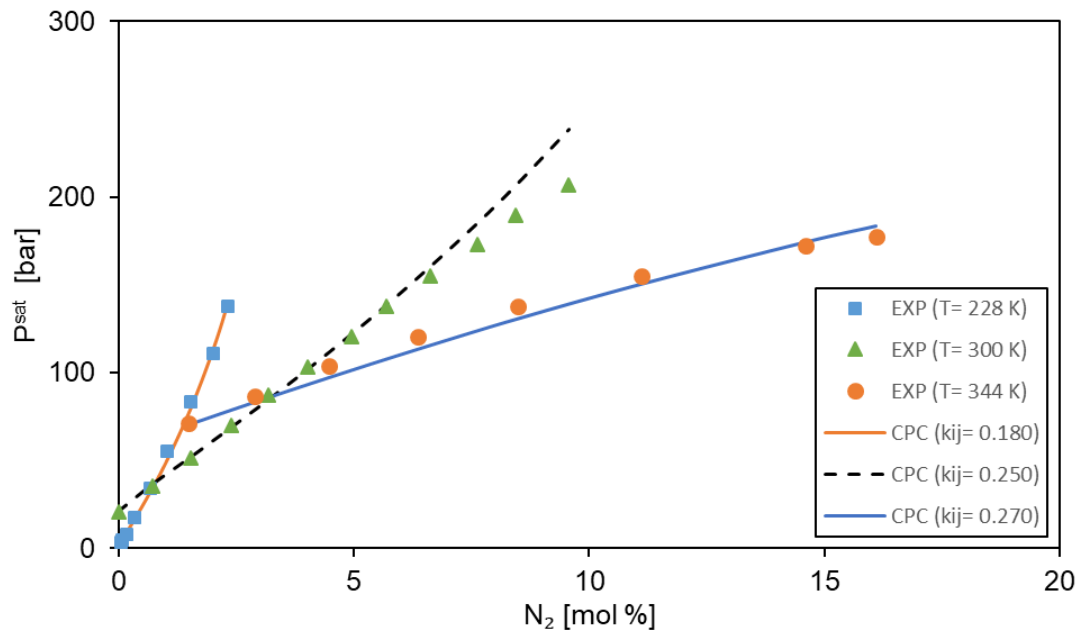
Figure C.12. Vapor-Liquid Equilibrium (VLE) for Nitrogen and Hydrogen Sulfide mixture with CPC at three different temperatures. Comparison of CPC calculations with different k_{ij} values with experimental data[77].